

Chiral extrapolation of baryon mass ratios

Peter C. Bruns, Ludwig Greil, and Andreas Schäfer

Institut für Theoretische Physik, Universität Regensburg, D-93040 Regensburg, Germany

(Dated: March 2, 2022)

Abstract

We analyze lattice data for octet baryon masses from the QCDSF collaboration employing manifestly covariant Baryon Chiral Perturbation Theory. It is shown that certain combinations of low-energy constants can be fixed more accurately than before from this data. We also examine the impact of this analysis on the pion-nucleon sigma term, and on the convergence properties of baryon mass expansions in the SU(3) symmetry limit.

PACS numbers:

arXiv:1209.0980v2 [hep-ph] 26 Feb 2013

I. INTRODUCTION

Three-flavor Baryon Chiral Perturbation Theory (BChPT) [1, 2] is an effective field theory for QCD in the low-energy regime where the lowest-lying meson-octet and the lowest-lying baryon octet (and possibly also the decuplet) are the relevant degrees of freedom.

It is now known for many years that chiral expansions derived from this framework are usually not under sufficient theoretical control because of an unsatisfying convergence behavior¹: higher-order corrections from chiral loops can in general not be guaranteed to be much smaller than the leading terms. The quark mass expansion around the three-flavor chiral limit converges slowly because the strange quark mass, m_s , is much larger than the light quark masses $m_\ell = m_{u,d}$, and induces sizeable kaon loop corrections to the leading tree level results. Detailed discussions on the convergence behavior of BChPT from various perspectives can be found in [3–12]. The essential point, however, can be seen immediately from a comparison of mass scales: while $\sqrt{2B_0m_\ell} \sim M_\pi \approx 140$ MeV is small compared to a typical hadronic scale of ~ 1 GeV, the three-flavor expansions can involve $\sqrt{2B_0m_s} =: M_{\bar{s}s} \approx 700$ MeV, which is not small compared to that reference scale. In fact, loop graphs involving the eta meson are only suppressed by an additional factor of $M_\eta/(4\pi F_0) \approx 0.5$, which can easily be compensated by additional prefactors (F_0 is the meson decay constant in the three-flavor chiral limit, while B_0 is related to the quark condensate in the same limit).

The problem is particularly urgent for chiral extrapolation formulae for lattice simulations. There, the meson masses are in general even larger than for physical quark masses. Consequently, the application of BChPT to such lattice data is not under satisfactory theoretical control. Though one can obtain fits that seem to describe the data fairly well, a stable determination of the corresponding low-energy constants (LECs) is not yet within reach, because the extracted values can be strongly affected by uncontrolled higher-order corrections. For some specific application, one might not even worry much about this, but one should recall that the main point of ChPT is to yield relations between many different observables, in terms of a limited set (at least at a fixed order in the low-energy expansion) of parameters. For example, the baryon mass in the chiral limit, m_0 , and its leading

¹ Of course, we are not concerned here with convergence in the strict mathematical sense, but with the reliability of theoretical predictions at low orders in perturbation theory.

quark mass corrections will unavoidably appear in practically *any* complete loop calculation in BChPT, in baryon form factors, meson-baryon scattering lengths, etc. Therefore, one should try to somehow control the higher-order loop corrections.

Many alternative ways to overcome this problem have been proposed in the literature, e.g. long-distance regularization [6], reordering and resummation schemes [7, 13], large- N_c -scaling arguments [14–17] and two-flavor expansions for hyperon properties [18, 19], each having its own merits. In this work, we stick to a standard scheme (evaluating the chiral loops employing infrared regularization [20]) and thus analyze the quark mass expansions of the baryon octet masses in a fashion closely following [21]. We refer to that reference for most of the corresponding technical details (see also [22]). For studies in different schemes, see e.g. [3, 23–34]. We have reproduced the complete one-loop ($\mathcal{O}(p^4)$) calculation in this covariant scheme. Our aim here is to put to use calculations like [21], by analyzing the lattice data presented in [35] which covers a quark mass region where all the masses of the pseudoscalar bosons are *smaller* than the physical eta mass, and to give improved estimates for LECs featuring in these calculations. We consider this a first and necessary step toward a controlled application of BChPT to such data sets. While in most three-flavor lattice simulations, the (large) strange quark mass is fixed², and the physical point is approached lowering m_ℓ (see e.g. [36, 37] for recent examples), the strategy in [35] is different: One simulates at a “symmetric point” where $m_\ell = m_s$, and then approaches the physical point increasing the quark mass difference, but keeping the average quark mass fixed. At the symmetric point, the pseudoscalar octet mesons all have the same mass of about 400 MeV, and on the trajectory to the physical point, the kaons and etas are lighter than observed in nature (there even exist some data points where the meson masses are all < 400 MeV at $m_s = m_\ell$). This is already a nice feature, but there is a second point that is probably even more important. In a surprisingly large region around the symmetric point, approximations neglecting all but linear symmetry-breaking effects were shown in [35] to yield a very good description of the data. In particular, quantities which do not receive linear symmetry-breaking contributions are observed to be very stable even down to the physical point (one example for such a quantity is the famous Gell-Mann-Okubo mass difference).

² In [36], the strange quark mass was 20% larger than the physical value, resulting in large kaon and eta masses, which makes the application of three-flavor chiral extrapolations even more problematic.

This behavior can not be understood from ChPT alone, but it puts tight constraints on certain combinations of LECs (e.g. by enforcing large cancellations in higher-order terms in the δm_ℓ -expansion of such quantities). It is convenient for the purpose of studying the symmetry-breaking effects separately to analyze certain baryon mass *ratios*, where a large factor with the dimension of mass (essentially the baryon mass at the symmetric point) cancels out. The behavior of these ratios can be very well described by BChPT (see our Fig. 5, and also [38] for a corresponding illustration). Here we want to exploit the advantages just mentioned for the determination of the LEC-combinations occurring in octet baryon masses, in the hope that this will help e.g. when analyzing lattice data for other quantities with the same strategy.

This paper is organized as follows: After briefly introducing some basic notation in sec. II, we collect the input from the purely mesonic sector in sec. III in some detail. This is necessary, because the quark-mass dependence of the masses of the pseudoscalar mesons is needed to rewrite the quark mass expansions of the baryon masses at $\mathcal{O}(p^4)$ in terms of the meson masses. We also include some simple examples of our strategy of analysis in this section. In sec. IV, we consider the result of the leading one-loop ($\mathcal{O}(p^3)$) calculation, to set the stage for the later developments. We also show some examples of a first numerical analysis, analyzing the experimental baryon masses. Sec. V completes the outline of our framework specifying the Lagrangians and diagrams entering at fourth chiral order. Readers who are only interested in the results for the baryon sector are invited to skip secs. III-V and directly continue with sec. VI, in which we discuss in detail the extrapolation functions we use, and which combinations of LECs can be extracted more accurately than before from the data we consider (and which can not). In a series of tables, we present our fit results, obtained with different fit strategies and input parameter sets. We discuss our results in sec. VII and give a short conclusion of our findings.

II. PRELIMINARIES

Throughout we work in the isospin limit and set the light quark masses to $m_u = m_d =: m_\ell$. In [35], the quark masses are varied along a trajectory T in the (m_ℓ, m_s) -space where the average quark mass $\bar{m} := \frac{1}{3}(2m_\ell + m_s)$ is kept fixed, while $\delta m_\ell = m_\ell - \bar{m}$ is varied. The aforesaid trajectory T connects the symmetric point, where $m_\ell = m_s = \bar{m}$, and the physical

point where the strange quark mass attains its physical value while $m_\ell = \frac{1}{2}(m_u + m_d)$.

To get familiar with the notation, let us consider the leading terms in the quark-mass expansion of the squares of the pseudo-Goldstone-boson masses. We have

$$\dot{M}_\pi^2 := 2B_0 m_\ell = 2B_0 \bar{m} + 2B_0 \delta m_\ell, \quad (1)$$

$$\dot{M}_K^2 := B_0(m_\ell + m_s) = 2B_0 \bar{m} - B_0 \delta m_\ell, \quad (2)$$

$$\dot{M}_\eta^2 := \frac{2}{3}B_0(m_\ell + 2m_s) = 2B_0 \bar{m} - 2B_0 \delta m_\ell. \quad (3)$$

Here B_0 is related to the quark condensate in the chiral limit, see e.g. [39]. The leading term of the pseudo-Goldstone-boson mass at the symmetric point is then found by setting $B_0 \delta m_\ell = 0$,

$$\dot{M}_\star^2 = 2B_0 \bar{m}. \quad (4)$$

Our notation is set up such that quantities in the chiral limit will be denoted by a subscript 0, while quantities at the symmetric point on T are marked with a \star .

In [35], it was noted that some specific combinations of hadron masses are very stable when varying the quark masses along T , compare e.g. Tab. 2 and Fig. 13 in that paper. Below, we list three of these combinations which are relevant for our present study:

$$X_N = \frac{1}{3}(m_N + m_\Sigma + m_\Xi) \approx 1150 \text{ MeV}, \quad (5)$$

$$X_\pi^2 = \frac{1}{3}(2M_K^2 + M_\pi^2) \approx (412 \text{ MeV})^2, \quad (6)$$

$$X_\eta^2 = \frac{1}{2}(M_\pi^2 + M_\eta^2) \approx (400 \text{ MeV})^2. \quad (7)$$

The experimental values are given in round brackets.

III. MESON MASSES AND DECAY CONSTANTS TO ONE LOOP

Meson masses

The one-loop expressions for the masses of the pions, kaons and the eta can be found e.g. in [39]. We give here the expansions of these formulae in terms of \bar{m} and δm_ℓ . The meson mass squared at the symmetric point is given (to one-loop accuracy) by

$$M_\star^2 = 2B_0 \bar{m} \left(1 + \frac{2B_0 \bar{m}}{(4\pi F_0)^2} \left(128\pi^2(-3L_4 - L_5 + 6L_6 + 2L_8) + \frac{2}{3} \log \left(\frac{\sqrt{2B_0 \bar{m}}}{\mu} \right) \right) \right). \quad (8)$$

The expansion of the meson masses in the symmetry-breaking parameter δm_ℓ reads

$$M_\pi^2 = M_\star^2 + (2B_0\delta m_\ell) \left(1 + \frac{2B_0\bar{m}}{(4\pi F_0)^2} \left(\frac{2}{3} + 2 \log \left(\frac{\sqrt{2B_0\bar{m}}}{\mu} \right) - 128\pi^2 (3L_4 + 2L_5 - 6L_6 - 4L_8) \right) \right) \\ + (B_0\delta m_\ell)^2 \left(\frac{5 + 8 \log \left(\frac{\sqrt{2B_0\bar{m}}}{\mu} \right) - 768\pi^2(L_5 - 2L_8)}{24\pi^2 F_0^2} \right), \quad (9)$$

$$M_K^2 = M_\star^2 + (2B_0\delta m_\ell) \left(-\frac{1}{2} - \frac{2B_0\bar{m}}{(4\pi F_0)^2} \left(\frac{1}{3} + \log \left(\frac{\sqrt{2B_0\bar{m}}}{\mu} \right) - 64\pi^2 (3L_4 + 2L_5 - 6L_6 - 4L_8) \right) \right) \\ + (B_0\delta m_\ell)^2 \left(\frac{1 + \log \left(\frac{\sqrt{2B_0\bar{m}}}{\mu} \right) - 96\pi^2(L_5 - 2L_8)}{12\pi^2 F_0^2} \right), \quad (10)$$

$$M_\eta^2 = M_\star^2 - (2B_0\delta m_\ell) \left(1 + \frac{2B_0\bar{m}}{(4\pi F_0)^2} \left(\frac{2}{3} + 2 \log \left(\frac{\sqrt{2B_0\bar{m}}}{\mu} \right) - 128\pi^2 (3L_4 + 2L_5 - 6L_6 - 4L_8) \right) \right) \\ - (B_0\delta m_\ell)^2 \left(\frac{8 + 12 \log \left(\frac{\sqrt{2B_0\bar{m}}}{\mu} \right) + 768\pi^2(L_5 - 12L_7 - 6L_8)}{24\pi^2 F_0^2} \right). \quad (11)$$

Consequently, we have for the combinations X_π^2, X_η^2 :

$$X_\pi^2 = \frac{1}{3}(2M_K^2 + M_\pi^2) = M_\star^2 + \frac{(B_0\delta m_\ell)^2}{24\pi^2 F_0^2} \left(3 + 4 \log \left(\frac{\sqrt{2B_0\bar{m}}}{\mu} \right) - 384\pi^2(L_5 - 2L_8) \right), \quad (12)$$

$$X_\eta^2 = \frac{1}{2}(M_\pi^2 + M_\eta^2) \\ = M_\star^2 - \frac{(B_0\delta m_\ell)^2}{48\pi^2 F_0^2} \left(3 + 4 \log \left(\frac{\sqrt{2B_0\bar{m}}}{\mu} \right) + 1536\pi^2(L_5 - 6L_7 - 4L_8) \right). \quad (13)$$

The low-energy constants L_i of course correspond to the renormalized constants $L_i^r(\mu)$ of [39]. In [35], instead of the quark mass difference $B_0\delta m_\ell$, the variable

$$\nu = \frac{M_\pi^2 - X_\pi^2}{X_\pi^2} \\ = \frac{2B_0\delta m_\ell}{M_\star^2} \left(1 + \frac{2B_0\bar{m}}{24\pi^2 F_0^2} \left(1 + 3 \log \left(\frac{\sqrt{2B_0\bar{m}}}{\mu} \right) - 192\pi^2(3L_4 + 2L_5 - 6L_6 - 4L_8) \right) \right) \\ + \frac{(2B_0\delta m_\ell)^2}{48\pi^2 F_0^2 M_\star^2} \left(1 + 2 \log \left(\frac{\sqrt{2B_0\bar{m}}}{\mu} \right) - 192\pi^2(L_5 - 2L_8) \right) \\ + \mathcal{O}(\bar{m}^2\delta m_\ell, \bar{m}(\delta m_\ell)^2, (\delta m_\ell)^3) \quad (14)$$

is used to parameterize the SU(3) symmetry breaking. Inverting this relation and again expanding up to the second order in the symmetry-breaking variable δm_ℓ , we get

$$2B_0\delta m_\ell = \nu M_\star^2 \left(1 - \frac{2B_0\bar{m}}{24\pi^2 F_0^2} \left(1 + 3 \log \left(\frac{\sqrt{2B_0\bar{m}}}{\mu} \right) - 192\pi^2(3L_4 + 2L_5 - 6L_6 - 4L_8) \right) \right) - \frac{(\nu M_\star^2)^2}{48\pi^2 F_0^2} \left(1 + 2 \log \left(\frac{\sqrt{2B_0\bar{m}}}{\mu} \right) - 192\pi^2(L_5 - 2L_8) \right), \quad (15)$$

where we have also truncated the chiral expansion of the coefficient functions in this series.

Decay constants

Similarly, the expansion of the decay constants is given by

$$F_\pi = F_\star - (B_0\delta m_\ell) \left(\frac{3 + 6 \log \left(\frac{\sqrt{2B_0\bar{m}}}{\mu} \right) - 256\pi^2 L_5}{32\pi^2 F_0} \right) + \mathcal{O}((\delta m_\ell)^2), \quad (16)$$

$$F_K = F_\star + (B_0\delta m_\ell) \left(\frac{3 + 6 \log \left(\frac{\sqrt{2B_0\bar{m}}}{\mu} \right) - 256\pi^2 L_5}{64\pi^2 F_0} \right) + \mathcal{O}((\delta m_\ell)^2), \quad (17)$$

$$F_\eta = F_\star + (B_0\delta m_\ell) \left(\frac{3 + 6 \log \left(\frac{\sqrt{2B_0\bar{m}}}{\mu} \right) - 256\pi^2 L_5}{32\pi^2 F_0} \right) + \mathcal{O}((\delta m_\ell)^2), \quad (18)$$

where

$$F_\star = F_0 \left(1 + \frac{2B_0\bar{m}}{(4\pi F_0)^2} \left(64\pi^2(3L_4 + L_5) - 3 \log \left(\frac{\sqrt{2B_0\bar{m}}}{\mu} \right) \right) \right) + \mathcal{O}(\bar{m}^2). \quad (19)$$

Note that if terms nonlinear in the symmetry-breaking variable are neglected, the combination

$$F_X := \frac{1}{3}(F_\pi + 2F_K) \quad (20)$$

is stable at that order.

Quark masses

For the sake of completeness, we also give an expression for the quantity $M_{\bar{s}s}^2 := 2B_0m_s$ in terms of the one-loop formulae for the meson masses:

$$\begin{aligned}
M_{\bar{s}s}^2 &= 2\dot{M}_K^2 - \dot{M}_\pi^2 = 2M_K^2 - M_\pi^2 \\
&+ \frac{1}{48\pi^2 F_0^2} \left(384\pi^2 (M_K^4(4L_4 + 2L_5 - 8L_6 - 4L_8) - M_\pi^4(L_4 + L_5 - 2L_6 - 2L_8)) \right. \\
&\left. + 3M_\pi^4 \log\left(\frac{M_\pi}{\mu}\right) - (3M_\eta^4 + 2M_\eta^2 M_\pi^2) \log\left(\frac{M_\eta}{\mu}\right) \right) + \mathcal{O}(M^6).
\end{aligned} \tag{21}$$

Keeping this quantity fixed, one can express the light quark mass dependence of the baryon masses through the pion mass dependence, using

$$\begin{aligned}
2B_0m_\ell &= M_\pi^2 \left(1 + \frac{1}{144\pi^2 F_0^2} \left(1152\pi^2 (M_\pi^2(2L_4 + L_5 - 4L_6 - 2L_8) + M_{\bar{s}s}^2(L_4 - 2L_6)) \right. \right. \\
&\left. \left. + (M_\pi^2 + 2M_{\bar{s}s}^2) \log\left(\frac{\sqrt{M_\pi^2 + 2M_{\bar{s}s}^2}}{\sqrt{3}\mu}\right) - 9M_\pi^2 \log\left(\frac{M_\pi}{\mu}\right) \right) \right) + \mathcal{O}(M^6).
\end{aligned} \tag{22}$$

Numerical analysis

For an overview on lattice determinations of the parameters F_0, L_i we refer to the recent discussion in [40]. We reproduce three sets of results in the table below. As central values in our numerical analysis, we adopt the set of parameters displayed in the first row (MILC2010). The other three parameter sets are used only for the error estimates of our results. The numerical values of the L_i are given at a renormalization scale of $\mu = 770$ MeV. At the order

TABLE I: Three parameter sets for the low-energy coefficients F_0, L_i .

F_0 (MeV)	$10^3 L_4$	$10^3 L_5$	$10^3 L_6$	$10^3 L_8$	Ref.
80.3 ± 6.0	-0.08 ± 0.60	0.98 ± 0.40	-0.02 ± 0.40	0.42 ± 0.30	MILC2010 [41]
78.3 ± 3.2	0.04 ± 0.14	0.84 ± 0.38	0.07 ± 0.11	0.36 ± 0.09	MILC2009 [42]
83.8 ± 6.4	-0.06 ± 0.10	1.45 ± 0.07	0.02 ± 0.05	0.62 ± 0.04	PACS2008 [36]

we are working, we can replace F_0 in eq. (8) by F_\star , see eq. (19). Given the observed stability of X_π , and the fact that this quantity is even used to set the scale for meson observables in

[35], we determine the parameter $2B_0\bar{m}$ from the requirement that $M_\star \stackrel{!}{=} X_\pi^{phys} = 412 \text{ MeV}$. We find

$$\sqrt{2B_0\bar{m}} \equiv \dot{M}_\star \stackrel{!}{=} (420 \pm 40) \text{ MeV}, \quad (23)$$

$$\Rightarrow F_\star = (112 \pm 15) \text{ MeV}. \quad (24)$$

We note that inserting the value for F_0 directly in eq. (8), one finds very similar values, $\dot{M}_\star = 428 \text{ MeV}$ and $F_\star = 112.5 \text{ MeV}$, while the experimental value for F_X is $F_X^{phys} = 105 \text{ MeV}$. As the one-loop effects discussed above enter our calculation of baryon masses formally at NNLO (meson masses) or even at two-loop order (decay constants), the estimates given in eqs. (23),(24) are sufficient for our purposes.

We also note that the fan plots for the meson masses shown in [35] can be nicely reproduced with the values of the LECs employed above, while X_π is indeed almost a constant along T . For this to be the case, one should expect from eq. (12) that

$$384\pi^2(L_5 - 2L_8) \approx 3 + 4 \log\left(\frac{420}{770}\right) \sim 0.58. \quad (25)$$

In fact, for our central values (MILC2010) we have

$$384\pi^2(L_5(\mu = 770 \text{ MeV}) - 2L_8(\mu = 770 \text{ MeV})) \sim 0.53, \quad (26)$$

so that terms in X_π quadratic in the symmetry breaking are indeed tiny. For X_η to be equally stable, we infer from eq. (13) that we should have $L_7 \sim -0.1 \cdot 10^{-3}$. In Fig. 1, we show a “fan plot” for the meson decay constants, i.e. we plot the ratios F_π/F_X and F_K/F_X as functions of the variable ν which parametrizes the SU(3) symmetry breaking, see eq. (15). The derivative at the symmetric point ($\nu = 0$) is essentially determined by the LEC L_5 , which we vary within the error according to MILC2010 to generate the bands around the central curves. One observes that the fan plot shows a linear behavior of the ratios with ν in the vicinity of the symmetric point, but some curvature is visible near the physical point, which seems to be necessary to reproduce the experimental values of F_π and F_K .

Inserting the experimental pion and kaon masses in eq. (21), one arrives at

$$M_{\bar{s}s} = (715 \pm 100) \text{ MeV}, \quad (27)$$

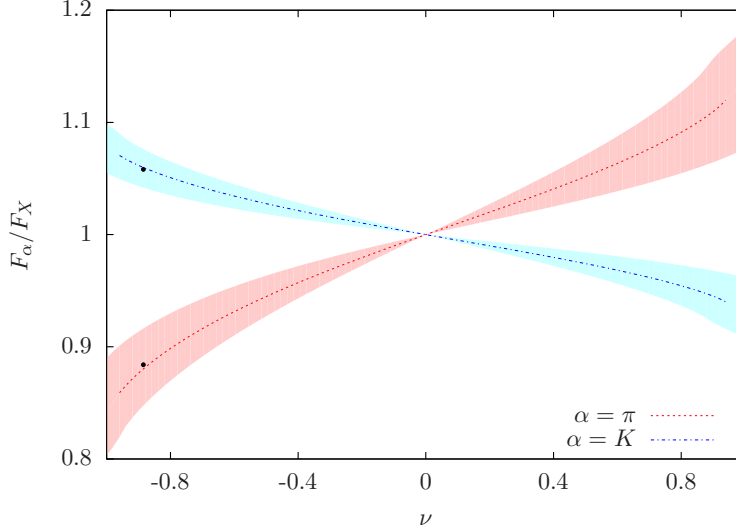


FIG. 1: A “fan plot” for the symmetry-breaking effects in the meson decay constants F_K and F_π . The black dots denote the experimental values.

where again we use the MILC2010 parameters as central values. The uncertainty due to the variation of the input parameters is somewhat larger than in eq. (23). We have a clear hierarchy

$$M_\pi \approx \sqrt{2B_0 m_\ell} < \sqrt{2B_0 \bar{m}} < \sqrt{2B_0 m_s} = M_{\bar{s}s}, \quad (28)$$

compare eqs. (23) and (27). While it is quite obvious that an expansion in $M_{\bar{s}s}$ (over a typical hadronic scale) will be ineffective, an expansion in \dot{M}_\star can be expected to work much better, since the expansion parameter is about 40% smaller.

IV. BARYON MASSES AT THIRD CHIRAL ORDER

From the relevant terms in the chiral Lagrangian,

$$\begin{aligned} \mathcal{L}_{\phi B} = & \langle \bar{B}(i\not{D} - m_0)B \rangle + \frac{D}{2} \langle \bar{B}\gamma^\mu\gamma_5\{u_\mu, B\} \rangle + \frac{F}{2} \langle \bar{B}\gamma^\mu\gamma_5[u_\mu, B] \rangle \\ & + b_0 \langle \bar{B}B \rangle \langle \chi_+ \rangle + b_D \langle \bar{B}\{\chi_+, B\} \rangle + b_F \langle \bar{B}[\chi_+, B] \rangle + \dots \end{aligned} \quad (29)$$

one derives the octet baryon masses to $\mathcal{O}(p^3)$ in BChPT (see e.g. [24])

$$m_N = m_0 - 4b_D \dot{M}_K^2 + 4b_F (\dot{M}_K^2 - \dot{M}_\pi^2) - 2b_0 (2\dot{M}_K^2 + \dot{M}_\pi^2) - \frac{-6DF (\dot{M}_\eta^3 + 2\dot{M}_K^3 - 3\dot{M}_\pi^3) + 9F^2 (\dot{M}_\eta^3 + 2\dot{M}_K^3 + \dot{M}_\pi^3) + D^2 (\dot{M}_\eta^3 + 10\dot{M}_K^3 + 9\dot{M}_\pi^3)}{96\pi F_0^2}, \quad (30)$$

$$m_\Lambda = m_0 + \frac{4}{3}b_D (-4\dot{M}_K^2 + \dot{M}_\pi^2) - 2b_0 (2\dot{M}_K^2 + \dot{M}_\pi^2) - \frac{9F^2 \dot{M}_K^3 + D^2 (\dot{M}_\eta^3 + \dot{M}_K^3 + 3\dot{M}_\pi^3)}{24\pi F_0^2}, \quad (31)$$

$$m_\Sigma = m_0 - 4b_D \dot{M}_\pi^2 - 2b_0 (2\dot{M}_K^2 + \dot{M}_\pi^2) - \frac{D^2 (\dot{M}_\eta^3 + 3\dot{M}_K^3 + \dot{M}_\pi^3) + 3F^2 (\dot{M}_K^3 + 2\dot{M}_\pi^3)}{24\pi F_0^2}, \quad (32)$$

$$m_\Xi = m_0 - 4b_D \dot{M}_K^2 - 4b_F (\dot{M}_K^2 - \dot{M}_\pi^2) - 2b_0 (2\dot{M}_K^2 + \dot{M}_\pi^2) - \frac{6DF (\dot{M}_\eta^3 + 2\dot{M}_K^3 - 3\dot{M}_\pi^3) + 9F^2 (\dot{M}_\eta^3 + 2\dot{M}_K^3 + \dot{M}_\pi^3) + D^2 (\dot{M}_\eta^3 + 10\dot{M}_K^3 + 9\dot{M}_\pi^3)}{96\pi F_0^2}, \quad (33)$$

from the second order quark mass insertions and the sunrise-type loop graph of Fig. 2. To this order, the mass of the eta can be eliminated by using the Gell-Mann-Okubo relation,

$$3\dot{M}_\eta^2 = 4\dot{M}_K^2 - \dot{M}_\pi^2. \quad (34)$$

Inserting $\dot{M}_K \rightarrow 495$ MeV and $\dot{M}_\pi \rightarrow 140$ MeV gives $\dot{M}_\eta \simeq 566$ MeV. In our numerical

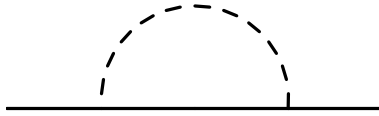


FIG. 2: Loop graph with axial meson-baryon vertices from the leading-order chiral Lagrangian, which yields the leading nonanalytic quark mass correction $\sim \sqrt{m_q^3}$. The full lines represent the baryons, while the dashed line represents the pseudoscalar meson π , K or η .

work, we shall use $D = \frac{3}{4}$, $F = \frac{1}{2}$ which is consistent with the available literature [43–46], see also [15]. It is difficult to reliably obtain these two axial coupling constants from a fit to baryon masses. In [15], values close to the expectation from phenomenology were obtained imposing a large- N_c counting and restricting the fit to certain mass combinations where the

singlet piece drops out. See also [33] for a similar result. For the above choice of D, F , the p^3 -terms cancel completely in the combination

$$\Delta_{DF} := \frac{1}{4} (12m_\Sigma - 4m_\Lambda - 5m_N - 3m_\Xi) = \frac{2}{3} (20b_D - 3b_F) \left(\dot{M}_K^2 - \dot{M}_\pi^2 \right) + \mathcal{O}(p^4). \quad (35)$$

This quantity vanishes in the SU(3) limit, however, it is not too small in the real world. Inserting the physical values for the baryon masses (averaging over isospin multiplets),

$$m_N^{phys} \simeq 939 \text{ MeV}, m_\Lambda^{phys} \simeq 1116 \text{ MeV}, m_\Sigma^{phys} \simeq 1190 \text{ MeV}, m_\Xi^{phys} \simeq 1318 \text{ MeV}, \quad (36)$$

gives $\Delta_{DF}^{phys} \simeq 292 \text{ MeV}$. Assuming that this choice for D, F is roughly correct, and that the $\mathcal{O}(p^4)$ terms are not too large, one would get $\frac{20}{3}b_D - b_F \sim 0.65/\text{GeV}$. It is known, however, that the BChPT expressions for the baryon masses only converge slowly at the physical point. Moreover, the numerical values of D and F are also a source of uncertainty. We shall therefore require only that the estimate for this combination of LECs is valid within a $\sim 50\%$ error,

$$\frac{0.3}{\text{GeV}} \lesssim \frac{20}{3}b_D - b_F \lesssim \frac{1}{\text{GeV}} \quad \text{for } D \approx \frac{3}{4}, F \approx \frac{1}{2}. \quad (37)$$

In contrast to Δ_{DF} , the well-known Gell-Mann-Okubo difference [47, 48]

$$\Delta_{GMO} := \frac{1}{4} (m_\Sigma + 3m_\Lambda - 2m_N - 2m_\Xi) = \frac{D^2 - 3F^2}{96\pi F_0^2} \left(4\dot{M}_K^3 - \dot{M}_\pi^3 - 3\dot{M}_\eta^3 \right) + \mathcal{O}(p^4). \quad (38)$$

is free of $\mathcal{O}(p^2)$ -corrections. Employing the input values $D = \frac{3}{4}$, $F = \frac{1}{2}$, $F_0 = 80.3 \text{ MeV}$, $\dot{M}_\pi = 140 \text{ MeV}$, $\dot{M}_K = 495 \text{ MeV}$, $\dot{M}_\eta = 566 \text{ MeV}$ yields $\Delta_{GMO} = 5.9 \text{ MeV} + \mathcal{O}(p^4)$, while $\Delta_{GMO}^{phys} \simeq 6.0 \text{ MeV}$ with the baryon masses used above. It seems that the higher-order corrections in this combination are very small: the effect is almost entirely given by the leading one-loop correction. The fact that Δ_{GMO} is so small numerically could be traced back to the fact that it is of order $(\delta m_\ell)^2$ in the symmetry-breaking variable.

Fitting the p^3 - expressions to the experimental baryon masses, with $D = \frac{3}{4}$, $F = \frac{1}{2}$, $m_0^{\text{eff}} := m_0 - 6b_0 X_\pi^2$ leads to the results presented in the table below. We vary the input parameter F_0 appearing in the $\mathcal{O}(q^3)$ -correction in a wide range to get a first impression of the uncertainty in these results. The convergence of the expansion of the baryon masses using these parameters is poor, however: For example, the third order correction to the nucleon mass is -423 MeV for $F_0 = 80.3 \text{ MeV}$. This is a very large correction, even if one expects a generic suppression factor of $\sim \frac{M_K}{4\pi F_0} \sim 0.5$ for each additional chiral order. We infer from these

F_0 (MeV)	m_0^{eff} (GeV)	b_D (GeV $^{-1}$)	b_F (GeV $^{-1}$)
70	2.279	-0.039	-0.912
80	2.024	-0.015	-0.747
112	1.617	0.024	-0.484
140	1.465	0.038	-0.386

results that a reliable determination of BChPT low-energy constants at (strange) quark masses higher than, or equal to, the value at the physical point is not feasible, due to much enhanced non-analytic loop corrections in this mass region. On the other hand, given that the above fit results can be regarded as a meaningful first approximation, we should at least expect the following pattern to be reproduced also in higher-order calculations:

1. $1 \text{ GeV} \lesssim m_0^{\text{eff}} < 3 \text{ GeV}$,
2. b_F is negative, $-1 \text{ GeV}^{-1} \lesssim b_F < 0 \text{ GeV}^{-1}$,
3. b_D is of significantly smaller magnitude than b_F .

Sigma term at third chiral order

The third-order formula for the pion-nucleon sigma term reads (see also [24]):

$$\sigma_{\pi N}(0) = -2\dot{M}_\pi^2(2b_0 + b_D + b_F) - \frac{\dot{M}_\pi^2}{64\pi F_0^2}(4\alpha_N^\pi \dot{M}_\pi + 2\alpha_N^K \dot{M}_K + \frac{4}{3}\alpha_N^\eta \dot{M}_\eta). \quad (39)$$

where

$$\alpha_N^\pi = \frac{9}{4}(D + F)^2, \quad \alpha_N^K = \frac{1}{2}(5D^2 - 6DF + 9F^2), \quad \alpha_N^\eta = \frac{1}{4}(D - 3F)^2. \quad (40)$$

Numerically, the third order correction gives a contribution of

$$-\dot{M}_\pi^2 \left(\frac{\dot{M}_K}{4\pi F_0} \right) \left(\frac{5.45}{\text{GeV}} \right) \sim -50 \text{ MeV} \quad (41)$$

at the physical point, to a positive quantity that is of the order 50 MeV ! This again casts strong doubts on the applicability of BChPT at the physical point to obtain reasonable predictions for sigma terms, without further input.

V. FOURTH ORDER CONTRIBUTIONS

At fourth chiral order, additional loop graphs have to be calculated. First, one has a graph of the same topology as the graph of Fig. 2, but with an additional quark mass insertion from the second order Lagrangian, proportional to $b_0, b_{D,F}$. This graph is shown on the l.h.s. of Fig. 3. In addition, there are tadpole-type contributions with vertices from the second order Lagrangian, accompanied by $b_0, b_{D,F}$ and also eight new constants $b_i, i = 1 \dots 4, 8 \dots 11$. There are also seven new contact terms $\sim d_i$ contributing to the masses at fourth order, they absorb divergences of the infrared-regularized loop integrals. The self-energy $\Sigma^{(n)}(\not{p})$ of n -th chiral order is then calculated directly from those graphs, and gives rise to the mass shifts $\Delta m_B^{(n')}$ at the different orders:

$$\begin{aligned} \Delta m_B^{(1)} &= 0, & \Delta m_B^{(2)} &= \Sigma^{(2)}, & \Delta m_B^{(3)} &= \Sigma^{(3)}(\not{p} = m_0), \\ \Delta m_B^{(4)} &= \Sigma^{(4)}(\not{p} = m_0) + \Sigma^{(2)} \frac{\partial \Sigma^{(3)}(\not{p})}{\partial \not{p}} \Big|_{\not{p}=m_0}. \end{aligned} \quad (42)$$

The calculation of the first graph in Fig. 3 is straightforward and does not introduce new

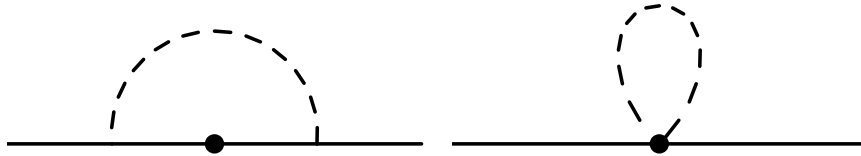


FIG. 3: Loop graphs giving contributions of fourth chiral order.

free parameters, so we will not discuss it further here (see e.g. Ref. [21]). In the following, we are concerned with the contact terms and the tadpole graphs, which involve new unknown couplings not present in a simple leading one-loop calculation. These new parameters can be grouped in two sets: one which will simply represent new free parameters to be determined in the fits, and one which will be fixed using input from other sources. Let us discuss both sets in turn.

Contact terms

We use the fourth order Lagrangian of Frink and Meißner [21],

$$\begin{aligned} \mathcal{L}_{\phi B}^{(4)} &= d_1 \langle \bar{B}[\chi_+, [\chi_+, B]] \rangle + d_2 \langle \bar{B}[\chi_+, \{\chi_+, B\}] \rangle + d_3 \langle \bar{B}\{\chi_+, \{\chi_+, B\}\} \rangle \\ &+ d_4 \langle \bar{B}\chi_+ \rangle \langle \chi_+ B \rangle + d_5 \langle \bar{B}[\chi_+, B] \rangle \langle \chi_+ \rangle + d_6 \langle \bar{B}B \rangle \langle \chi_+ \rangle \langle \chi_+ \rangle + d_7 \langle \bar{B}B \rangle \langle \chi_+^2 \rangle. \end{aligned} \quad (43)$$

The contact terms give the following contributions to the baryon masses:

$$\begin{aligned}
m_N^{(ct)} &= m_\star^{(ct)} + B_0 \delta m_\ell (4(b_D - 3b_F) - 16B_0 \bar{m} (6d_2 - 4d_3 + 9d_5)) \\
&\quad - 16(B_0 \delta m_\ell)^2 (9d_1 - 3d_2 + d_3 + 6d_7) , \\
m_\Lambda^{(ct)} &= m_\star^{(ct)} + 8B_0 \delta m_\ell (b_D + 16B_0 \bar{m} d_3) - 96(B_0 \delta m_\ell)^2 (2d_3 + d_4 + d_7) , \\
m_\Sigma^{(ct)} &= m_\star^{(ct)} - 8B_0 \delta m_\ell (b_D + 16B_0 \bar{m} d_3) - 16(B_0 \delta m_\ell)^2 (4d_3 + 6d_7) , \\
m_\Xi^{(ct)} &= m_\star^{(ct)} + B_0 \delta m_\ell (4(b_D + 3b_F) + 16B_0 \bar{m} (6d_2 + 4d_3 + 9d_5)) \\
&\quad - 16(B_0 \delta m_\ell)^2 (9d_1 + 3d_2 + d_3 + 6d_7) ,
\end{aligned} \tag{44}$$

where $m_\star^{(ct)} = -4B_0 \bar{m} (3b_0 + 2b_D) - 16(B_0 \bar{m})^2 (4d_3 + 9d_6 + 3d_7)$.

We also recall that the combination X_N has no linear symmetry-breaking terms. In particular,

$$X_N^{(ct)} = m_\star^{(ct)} - 32(B_0 \delta m_\ell)^2 (3d_1 + d_3 + 3d_7) . \tag{45}$$

In the contact term contributions linear in the symmetry-breaking, only the combinations $\tilde{b}_D := b_D + 16B_0 \bar{m} d_3$ and $\tilde{b}_F := b_F + 4B_0 \bar{m} (2d_2 + 3d_5)$ enter. While $d_{2,3}$ also enter the terms quadratic in δm_ℓ , we can not determine d_5 from the fan plots at the order we are working (the tadpole contribution involving b_F is already of fourth order in the chiral counting). Moreover, the LECs b_0 and d_6 only enter in the combination

$$m_\star = m_0 - 12B_0 \bar{m} (b_0 + 12B_0 \bar{m} d_6) + \dots , \tag{46}$$

so these two parameters can also not be determined individually from the fan plots alone (again, the shift proportional to d_6 would be of higher chiral order in the tadpole graph involving b_0). For a later application, we also give the contact term contribution to the pion-nucleon sigma term. It is computed here employing the Hellmann-Feynman-theorem,

$$\begin{aligned}
\sigma_{\pi N}^{(ct)}(0) &= m_\ell \frac{\partial m_N^{(ct)}}{\partial m_\ell} = m_\ell \frac{\partial}{\partial m_\ell} \left(m_\star^{(ct)} + (B_0 \delta m_\ell) m_N^{(1,ct)} + (B_0 \delta m_\ell)^2 m_N^{(2,ct)} \right) \\
&= m_\ell \frac{2}{3} \frac{\partial m_\star^{(ct)}}{\partial \bar{m}} + \frac{1}{3} B_0 m_\ell m_N^{(1,ct)} + (B_0 \delta m_\ell) \frac{2}{3} \left(m_\ell \frac{\partial m_N^{(1,ct)}}{\partial \bar{m}} + B_0 m_\ell m_N^{(2,ct)} \right) .
\end{aligned} \tag{47}$$

Inserting the expressions from eq. (44), we find

$$\begin{aligned}
\sigma_{\pi N}^{(ct)}(0) &= -2B_0 m_\ell \left(4b_0 + 2b_D + 2b_F + \frac{32}{3} B_0 \bar{m} (4d_3 + 9d_6 + 3d_7) + \frac{8}{3} B_0 \bar{m} (6d_2 - 4d_3 + 9d_5) \right. \\
&\quad \left. + 16(B_0 \delta m_\ell) (3d_1 + d_2 - d_3 + 3d_5 + 2d_7) \right) .
\end{aligned} \tag{48}$$

Tadpole graphs

The second order Lagrangian we employ here differs slightly from the one given in [21] because since then one further term could be eliminated [49]. The Lagrangian is then given by

$$\begin{aligned}
\mathcal{L}_{\phi B}^{(2)} = & b_{D/F} \langle \bar{B} [\chi_+, B]_{\pm} \rangle + b_0 \langle \bar{B} B \rangle \langle \chi_+ \rangle \\
& + b_{1/2} \langle \bar{B} [u_\mu, [u^\mu, B]_{\mp}] \rangle + b_3 \langle \bar{B} \{u_\mu, \{u^\mu, B\}\} \rangle + b_4 \langle \bar{B} B \rangle \langle u_\mu u^\mu \rangle \\
& + i \left(b_{5/6} \langle \bar{B} \sigma^{\mu\nu} [[u_\mu, u_\nu], B]_{\mp} \rangle + b_7 \langle \bar{B} \sigma^{\mu\nu} u_\mu \rangle \langle u_\nu B \rangle \right) \\
& + \frac{i b_{8/9}}{2m_0} \left(\langle \bar{B} \gamma^\mu [u_\mu, [u_\nu, [D^\nu, B]]_{\mp}] \rangle + \langle \bar{B} \gamma^\mu [D_\nu, [u^\nu, [u_\mu, B]]_{\mp}] \rangle \right) \\
& + \frac{i b_{10}}{2m_0} \left(\langle \bar{B} \gamma^\mu \{u_\mu, \{u_\nu, [D^\nu, B]\}\} \rangle + \langle \bar{B} \gamma^\mu [D_\nu, \{u^\nu, \{u_\mu, B\}\}] \rangle \right) \\
& + \frac{i b_{11}}{2m_0} \left(2 \langle \bar{B} \gamma^\mu [D_\nu, B] \rangle \langle u_\mu u^\nu \rangle + \langle \bar{B} \gamma^\mu B \rangle \langle [D_\nu, u_\mu] u^\nu + u_\mu [D_\nu, u^\nu] \rangle \right).
\end{aligned} \tag{49}$$

This form has also been used in [50, 51], and we shall also take the numerical values of the LECs b_{1-4} , b_{8-11} from the latter references. Note, however, that in those references, the chiral potential derived from the above Lagrangian is iterated to infinite order in a coupled-channel Bethe-Salpeter equation, introducing a model-dependent uncertainty not controlled within strict ChPT. To estimate the impact of this uncertainty on our results, we perform all our fits with three different parameter sets from meson-baryon scattering (set 1-3). In addition, we also add one parameter set where we take all b_{1-11} to vanish (set 4). The four parameter sets are collected in the table below (in GeV^{-1}). b_{5-7} do not

TABLE II: Four parameter sets for the low-energy coefficients b_{1-4} , b_{8-11} .

set	b_1	b_2	b_3	b_4	b_8	b_9	b_{10}	b_{11}	Ref.
1	-0.082	-0.118	-1.890	-0.215	0.609	-0.633	1.920	-0.919	[50]
2	-0.126	-0.139	-2.227	-0.288	0.610	-0.677	2.027	-0.847	[51]
3	-0.014	-0.207	-1.063	-1.312	0.272	-0.483	1.054	0.328	[51]
4	0	0	0	0	0	0	0	0	-

contribute to the baryon masses at one-loop order. We shall not write out the full tadpole contributions to the baryon masses. The corresponding contributions to the terms linear in

the symmetry-breaking δm_ℓ and to the baryon mass in the symmetry limit, m_\star , can be read off from eqs. (69) and (71).

Renormalization

The infrared regularized loop integrals still contain UV divergences as $d \rightarrow 4$, proportional to

$$L := \frac{\mu^{d-4}}{16\pi^2} \left(\frac{1}{d-4} - \frac{1}{2} [\ln(4\pi) + \Gamma'(1) + 1] \right). \quad (50)$$

The couplings $b_{0,D,F}$ do not have to absorb divergences from the infrared regularized loop graphs. At third order, there are no counterterms contributing to the baryon masses, and therefore also no divergences. The divergences of the infrared singular parts of the loop integrals at fourth order can be absorbed by the following renormalization prescription for the counterterms d_i :

$$d_i = \gamma_i^{\text{IR}} L + d_i^{(r)}(\mu), \quad (51)$$

with

$$\begin{aligned} \gamma_1^{\text{IR}} &= \frac{1}{72F_0^2} \left(b_D(14 + 69D^2 + 81F^2) + 162b_F DF + \frac{D^2 - 3F^2}{m_0} - (12b_1 - 4b_3 + 3b_8 - b_{10}) \right), \\ \gamma_2^{\text{IR}} &= \frac{1}{48F_0^2} \left(120b_D DF + b_F(4 + 60D^2 + 108F^2) + \frac{6DF}{m_0} + 3(4b_2 + b_9) \right), \\ \gamma_3^{\text{IR}} &= \frac{1}{48F_0^2} \left(6b_D(4 + 13D^2 + 9F^2) + 108b_F DF + \frac{3(D^2 - 3F^2)}{m_0} - (36b_1 + 4b_3 + 9b_8 + b_{10}) \right), \\ \gamma_4^{\text{IR}} &= \frac{1}{72F_0^2} \left(-4b_D(11 + 72D^2) - \frac{9(D^2 - 3F^2)}{m_0} + 108b_1 - 4b_3 + 27b_8 - b_{10} \right), \\ \gamma_5^{\text{IR}} &= \frac{1}{72F_0^2} \left(44b_F - \frac{26DF}{m_0} - 13(4b_2 + b_9) \right), \\ \gamma_6^{\text{IR}} &= \frac{1}{432F_0^2} \left(264b_0 + b_D(132 - 144D^2) - \frac{35D^2 + 27F^2}{m_0} \right. \\ &\quad \left. - (108b_1 + 140b_3 + 264b_4 + 27b_8 + 35b_{10} + 66b_{11}) \right), \\ \gamma_7^{\text{IR}} &= \frac{1}{144F_0^2} \left(120b_0 + b_D(28 - 24(7D^2 + 9F^2)) - 432b_F DF - \frac{17D^2 + 9F^2}{m_0} \right. \\ &\quad \left. - (36b_1 + 68b_3 + 120b_4 + 9b_8 + 17b_{10} + 30b_{11}) \right). \end{aligned} \quad (52)$$

We can then define scale-independent quantities \bar{d}_i by

$$d_i^{(r)}(\mu) = \bar{d}_i + \frac{\gamma_i^{\text{IR}}}{16\pi^2} \log\left(\frac{m_0}{\mu}\right). \quad (53)$$

VI. ANALYSIS OF FAN PLOT DATA

The main objective of this study is the analysis of the fan plot data collected in Tab. 22 and Fig. 20 of [35]. The following ratios of baryon masses are considered,

$$f_B := \frac{m_B}{X_N} \quad \text{for } B = N, \Lambda, \Sigma, \Xi, \quad (54)$$

see also eq. (5) for the definition of X_N . At the point on the symmetric line where $m_\ell = m_s = \bar{m}$, we have $f_B = \frac{m_\star}{m_\star} = 1$ and $X_\pi = M_\star = 412 \text{ MeV}$. The symmetry breaking is then switched on by varying δm_ℓ for fixed \bar{m} . For the data points with the greatest distance from the symmetric point, we compute $\nu = -0.692$ from eq. (14). The meson masses at this point are $M_\pi \approx 229 \text{ MeV}$, $M_K \approx 477 \text{ MeV}$ and (using eq. (34)) $M_\eta \approx 535 \text{ MeV}$. All meson masses stay well below the experimental eta mass, in contrast to other lattice data sets (with m_s fixed instead of \bar{m}), where the meson masses are usually *larger* than the meson masses in the real world. There is therefore good reason to believe that the chiral extrapolation formulae provided by three-flavor BChPT will work better when applied to the present data set than in the usual applications, though meson masses of $\sim 400 \text{ MeV}$ are probably still too high to assure a proper convergence behavior of the chiral expansions in general. Another indication of a better behavior of the quantities considered here is the observation (made in [35]) that finite-volume effects, which are mainly generated by the chiral loops, tend to cancel out in the baryon mass ratios f_B . Here we only remark that finite volume effects might still be non-negligible for the data in question, and deserve further study. It is also interesting to note that, employing large- N_c arguments and Heavy-Baryon ChPT, it was shown in [15] that the poor convergence behavior of the three-flavor chiral extrapolations could be traced back to the flavor-singlet sector, considering in particular the mass relation called R_1 in the latter reference. This again suggests that it might be a good idea to factor out a convenient flavor-singlet quantity (in our case, X_N) as is done in the baryon mass ratios relevant for the fan plots. In this section, we will see that certain combinations of low-energy constants can already be extracted quite reliably from the fan plot data for the ratios f_B , namely, the LEC combinations which parameterize the leading symmetry-breaking contributions to

the baryon masses. We consider this as a first and necessary step toward a theoretically controlled application of BChPT formulae to lattice data. We also make an attempt to determine the remaining LECs occurring in the baryon mass extrapolations, however, the constants parameterizing the singlet contributions can only be roughly estimated.

Though we shall use the full one-loop BChPT expressions for the baryon masses in the ratios f_B in the end, it is instructive to consider the expansion of the latter ratios in the variable δm_ℓ parameterizing the symmetry breaking. This will make clear which subsets and combinations of LECs can be more accurately determined than before, and what the qualifications and sources of uncertainties for the various determinations are.

Expansion of mass ratios f_B

Employing the full one-loop ChPT calculation of the baryon masses, we are sensitive only up to terms $(\delta m_\ell)^k \bar{m}^{2-k}$, while higher order terms will be modified by terms on the two-loop level. Therefore, the following equations are to be understood as resulting from a double expansion: the chiral expansion, on the one hand, and the expansion in δm_ℓ , on the other hand. One finds

$$f_B = 1 + (B_0 \delta m_\ell) f_B^{(1)} + (B_0 \delta m_\ell)^2 f_B^{(2)} + \mathcal{O}((\delta m_\ell)^3), \quad (55)$$

where

$$f_N^{(1)} = \frac{4(b_D - 3b_F)}{m_0} - \sqrt{2B_0 \bar{m}} \frac{3(D^2 + 10DF - 3F^2)}{32m_0 \pi F_0^2} + (16B_0 \bar{m}) \left(\frac{(3b_0 + 2b_D)(b_D - 3b_F)}{m_0^2} - \frac{6d_2 - 4d_3 + 9d_5}{m_0} + \dots \right) + \mathcal{O}(\bar{m}^{3/2}), \quad (56)$$

$$f_\Lambda^{(1)} = \frac{8b_D}{m_0} - \sqrt{2B_0 \bar{m}} \frac{3(D^2 - 3F^2)}{16m_0 \pi F_0^2} + (16B_0 \bar{m}) \left(\frac{2(3b_0 + 2b_D)b_D}{m_0^2} + \frac{8d_3}{m_0} + \dots \right) + \mathcal{O}(\bar{m}^{3/2}), \quad (57)$$

$$f_\Sigma^{(1)} = -\frac{8b_D}{m_0} + \sqrt{2B_0 \bar{m}} \frac{3(D^2 - 3F^2)}{16m_0 \pi F_0^2} - (16B_0 \bar{m}) \left(\frac{2(3b_0 + 2b_D)b_D}{m_0^2} + \frac{8d_3}{m_0} + \dots \right) + \mathcal{O}(\bar{m}^{3/2}), \quad (58)$$

$$f_\Xi^{(1)} = \frac{4(b_D + 3b_F)}{m_0} - \sqrt{2B_0 \bar{m}} \frac{3(D^2 - 10DF - 3F^2)}{32m_0 \pi F_0^2} + (16B_0 \bar{m}) \left(\frac{(3b_0 + 2b_D)(b_D + 3b_F)}{m_0^2} + \frac{6d_2 + 4d_3 + 9d_5}{m_0} + \dots \right) + \mathcal{O}(\bar{m}^{3/2}), \quad (59)$$

and

$$f_N^{(2)} = -\frac{D^2 + 18DF - 3F^2}{128\sqrt{2B_0\bar{m}}m_0\pi F_0^2} - 16\frac{3d_1 - 3d_2 - d_3}{m_0} + \dots + \mathcal{O}(\bar{m}^{1/2}), \quad (60)$$

$$f_\Lambda^{(2)} = -\frac{10(D^2 - 3F^2)}{128\sqrt{2B_0\bar{m}}m_0\pi F_0^2} + 32\frac{3d_1 - 5d_3 - 3d_4}{m_0} + \dots + \mathcal{O}(\bar{m}^{1/2}), \quad (61)$$

$$f_\Sigma^{(2)} = \frac{2(D^2 - 3F^2)}{128\sqrt{2B_0\bar{m}}m_0\pi F_0^2} + 32\frac{3d_1 - d_3}{m_0} + \dots + \mathcal{O}(\bar{m}^{1/2}), \quad (62)$$

$$f_\Xi^{(2)} = -\frac{D^2 - 18DF - 3F^2}{128\sqrt{2B_0\bar{m}}m_0\pi F_0^2} - 16\frac{3d_1 + 3d_2 - d_3}{m_0} + \dots + \mathcal{O}(\bar{m}^{1/2}). \quad (63)$$

The dots stand for corrections from loop graphs of fourth chiral order, which we do not display explicitly here. Let us concentrate first on the contribution from the contact terms.

We make the following observations:

1. $f_\Sigma^{(1)} = -f_\Lambda^{(1)}$,
2. $f_N^{(n)} + f_\Sigma^{(n)} + f_\Xi^{(n)} = 0$,
3. the baryon mass m_0 only appears in combination with low-energy constants, in the ratios $D/\sqrt{m_0}$, $F/\sqrt{m_0}$, b_i/m_0 , d_i/m_0 ,
4. the LEC d_7 does not appear at this order in the double expansion of the ratios.

The last two items would lead to problems when only using the fan plots and ratios f_B in the fitting procedure: First, since terms of order $(\delta m_\ell)^3$ and higher are expected to be small in most parts of the fan plots, it is very likely that a stable determination of d_7 would be difficult. Second, we would like to use the values of D, F, b_{1-4}, b_{8-11} directly as input, and the baryon mass in the chiral limit, m_0 , is not accurately known. What is more or less accurately known, however, is the baryon mass at the symmetric point,

$$m_\star = m_0 - 4B_0\bar{m}(3b_0 + 2b_D) + \mathcal{O}(\bar{m}^{3/2}), \quad (64)$$

for reasons discussed in the next subsection. We can eliminate m_0 in favor of m_\star . Moreover, we can replace F_0 by F_\star (see eq. (19)) at the order we are working. These replacements are rather natural when expanding in the symmetry breaking around the point $m_\ell = m_s = \bar{m}$. Doing this, the previous expansions read after this slight reordering (in terms of $\tilde{b}_{D,F}$ defined

above):

$$\begin{aligned}
f_N^{(1)} &= \frac{4(\tilde{b}_D - 3\tilde{b}_F)}{m_\star} - \sqrt{2B_0\bar{m}} \frac{3(D^2 + 10DF - 3F^2)}{32m_\star\pi F_\star^2} \\
&\quad - \frac{4B_0\bar{m}}{(4\pi F_\star)^2} \left[\frac{\tilde{b}_D - 3\tilde{b}_F}{m_\star} \left(\frac{5}{3} + 8 \log \left(\frac{\sqrt{2B_0\bar{m}}}{\mu} \right) \right) \right. \\
&\quad + \frac{2\tilde{b}_D}{m_\star} (13D^2 - 30DF + 9F^2) \left(\frac{1}{3} + \log \left(\frac{\sqrt{2B_0\bar{m}}}{\mu} \right) \right) \\
&\quad - \frac{6\tilde{b}_F}{m_\star} (5D^2 - 6DF + 9F^2) \left(\frac{1}{3} + \log \left(\frac{\sqrt{2B_0\bar{m}}}{\mu} \right) \right) \\
&\quad \left. + \frac{D^2 + 10DF - 3F^2}{m_\star^2} \left(\frac{3}{4} + \log \left(\frac{\sqrt{2B_0\bar{m}}}{\mu} \right) \right) \right] + \mathcal{T}_N^{(1)} + \mathcal{O}(\bar{m}^{3/2}), \tag{65}
\end{aligned}$$

$$\begin{aligned}
f_\Lambda^{(1)} &= \frac{8\tilde{b}_D}{m_\star} - \sqrt{2B_0\bar{m}} \frac{3(D^2 - 3F^2)}{16m_\star\pi F_\star^2} - \frac{4B_0\bar{m}}{(4\pi F_\star)^2} \left[\frac{2\tilde{b}_D}{m_\star} \left(\frac{5}{3} + 8 \log \left(\frac{\sqrt{2B_0\bar{m}}}{\mu} \right) \right) \right. \\
&\quad + \frac{4\tilde{b}_D}{m_\star} (13D^2 + 9F^2) \left(\frac{1}{3} + \log \left(\frac{\sqrt{2B_0\bar{m}}}{\mu} \right) \right) + \frac{72\tilde{b}_F}{m_\star} DF \left(\frac{1}{3} + \log \left(\frac{\sqrt{2B_0\bar{m}}}{\mu} \right) \right) \\
&\quad \left. + \frac{2(D^2 - 3F^2)}{m_\star^2} \left(\frac{3}{4} + \log \left(\frac{\sqrt{2B_0\bar{m}}}{\mu} \right) \right) \right] + \mathcal{T}_\Lambda^{(1)} + \mathcal{O}(\bar{m}^{3/2}), \tag{66}
\end{aligned}$$

$$f_\Sigma^{(1)} = -f_\Lambda^{(1)}, \tag{67}$$

$$f_\Xi^{(1)} = -(f_N^{(1)} + f_\Sigma^{(1)}), \tag{68}$$

while the formulae for $f_B^{(2)}$ just change in that $m_0 \rightarrow m_\star$ at the chiral order we are working. $\mathcal{T}_B^{(1)}$ stand for contributions from tadpole graphs proportional to b_{1-4}, b_{8-11} . These are given below. We see that from the derivative of the ratios at the symmetric point, we can determine two parameters only, due to the symmetry constraints in (i) and (ii), namely $\tilde{b}_{D,F}$. From the tadpole contributions to the $f_B^{(1)}$,

$$\begin{aligned}
\mathcal{T}_N^{(1)} &= \frac{4B_0\bar{m}}{3(4\pi F_\star)^2} \left[\frac{9b_1 - 15b_2 + b_3}{m_\star} \left(1 + 4 \log \left(\frac{\sqrt{2B_0\bar{m}}}{\mu} \right) \right) + \frac{9b_8 - 15b_9 + b_{10}}{m_\star} \log \left(\frac{\sqrt{2B_0\bar{m}}}{\mu} \right) \right], \\
\mathcal{T}_\Lambda^{(1)} &= \frac{8B_0\bar{m}}{3(4\pi F_\star)^2} \left[\frac{9b_1 + b_3}{m_\star} \left(1 + 4 \log \left(\frac{\sqrt{2B_0\bar{m}}}{\mu} \right) \right) + \frac{9b_8 + b_{10}}{m_\star} \log \left(\frac{\sqrt{2B_0\bar{m}}}{\mu} \right) \right], \tag{69}
\end{aligned}$$

we can see that $b_{2,9}$ enter there only for N, Ξ , while the combinations $9b_1 + b_3, 9b_8 + b_{10}$ enter for all four baryons.

Expansion of X_N

The above ratios f_B are all normalized to $X_N := \frac{1}{3}(m_N + m_\Sigma + m_\Xi)$. This combination was shown in [35] to be practically constant along a trajectory with constant \bar{m} , and thus approximately equal to $m_\star^{num} = 1150$ MeV for the choice of \bar{m} corresponding to the experimental hadron masses. Subsequently, X_N was even used to set the scale in the simulations leading to the fan plot for the baryon masses. Employing our ChPT formulae, the flat behavior of X_N is not automatically guaranteed, but should be enforced in the fitting procedure. To see how this can be done, we write down the expansion of X_N in the symmetry-breaking variable δm_ℓ :

$$X_N = m_\star + (B_0 \delta m_\ell)^2 X_N^{(2)} + \mathcal{O}((\delta m_\ell)^3), \quad (70)$$

with

$$\begin{aligned} m_\star &= m_0 - 4B_0 \bar{m} (3b_0 + 2b_D) - (2B_0 \bar{m})^{3/2} \frac{(5D^2 + 9F^2)}{24\pi F_\star^2} \\ &+ \frac{(2B_0 \bar{m})^2}{3(4\pi F_\star)^2} \left[32(3b_0 + 2b_D) \log \left(\frac{\sqrt{2B_0 \bar{m}}}{\mu} \right) - 8(9b_1 + 7b_3 + 12b_4) \log \left(\frac{\sqrt{2B_0 \bar{m}}}{\mu} \right) \right. \\ &- 2(9b_8 + 7b_{10} + 12b_{11}) \left(\log \left(\frac{\sqrt{2B_0 \bar{m}}}{\mu} \right) - \frac{1}{4} \right) - 12(4\pi F_\star)^2 (4d_3 + 9d_6 + 3d_7) \\ &\left. - \frac{(5D^2 + 9F^2)}{m_0} \left(1 + 2 \log \left(\frac{\sqrt{2B_0 \bar{m}}}{\mu} \right) \right) \right] + \mathcal{O}(\bar{m}^{5/2}), \end{aligned} \quad (71)$$

and

$$\begin{aligned} X_N^{(2)} &= -\frac{3(D^2 + 2F^2)}{16\pi F_\star^2 \sqrt{2B_0 \bar{m}}} - 32(3d_1 + d_3 + 3d_7) + \frac{5b_0}{\pi^2 F_\star^2} \left(\frac{3}{4} + \log \left(\frac{\sqrt{2B_0 \bar{m}}}{\mu} \right) \right) \\ &+ \frac{b_D}{6\pi^2 F_\star^2} \left(2D^2 \left(5 + 6 \log \left(\frac{\sqrt{2B_0 \bar{m}}}{\mu} \right) \right) + 15 + 20 \log \left(\frac{\sqrt{2B_0 \bar{m}}}{\mu} \right) \right) \\ &- \frac{(12b_1 + 8b_3 + 15b_4)}{12\pi^2 F_\star^2} \left(3 + 4 \log \left(\frac{\sqrt{2B_0 \bar{m}}}{\mu} \right) \right) \\ &- \frac{(12b_8 + 8b_{10} + 15b_{11})}{24\pi^2 F_\star^2} \left(1 + 2 \log \left(\frac{\sqrt{2B_0 \bar{m}}}{\mu} \right) \right) \\ &- \frac{D^2 + 2F^2}{2m_0 \pi^2 F_\star^2} \left(\frac{5}{4} + \log \left(\frac{\sqrt{2B_0 \bar{m}}}{\mu} \right) \right) + \mathcal{O}(\bar{m}^{1/2}). \end{aligned} \quad (72)$$

Here, the LEC d_7 shows up at order \bar{m}^2 and $(\delta m_\ell)^2$, respectively. The baryon mass in the chiral limit, m_0 , and the combinations of LECs appearing here will be determined in the next section from the behavior of $m_\star(\bar{m})$, for which some lattice data points with $300 \text{ MeV} < M_\star < 500 \text{ MeV}$ exist. We repeat that we dismiss any lattice data involving meson masses much above 500 MeV.

Linear fits to the fan plots

As a first step, we perform a linearized fit to the fan plot data only. Only the LEC-combinations that enter terms linear in the symmetry breaking can be safely determined from such fits. As shown above, in a full one-loop calculation in ChPT, these are the combinations $\tilde{b}_{D,F}$. As an additional constraint, we impose that the mass combination X_N does not deviate much from the physical value ~ 1150 MeV. Approximating

$$\begin{aligned} f_B &\approx 1 + \nu f_B^{(1,\nu)}, \\ X_N &\approx m_\star + \nu^2 X_N^{(2,\nu)}, \end{aligned} \tag{73}$$

using eqs. (68) and (15), and truncating the coefficients after $\mathcal{O}((2B_0\bar{m})^2)$, we can determine the following four combinations of LECs from such fits:

$$\begin{aligned} \tilde{b}_D &= b_D + 16B_0\bar{m}d_3, & \tilde{b}_F &= b_F + 4B_0\bar{m}(2d_2 + 3d_5) \equiv b'_F + 8B_0\bar{m}d_2, \\ \tilde{b}_0 &= b_0 - 2B_0\bar{m} \left(\frac{8}{3}d_3 - 6d_6 - 2d_7 \right), & \tilde{d}_7 &= d_1 + \frac{1}{3}d_3 + d_7. \end{aligned} \tag{74}$$

The loop functions are evaluated at a scale $\mu = 1150$ MeV. We have checked that, given the running of the coupling constants with μ from eq. (53), the masses are independent of the choice of scale when truncating after $\mathcal{O}(p^4)$.

In our numerical analysis, we use $2B_0\bar{m} = (420 \text{ MeV})^2$ in order to fix the meson mass at the symmetric point, M_\star , to 412 MeV for the set of meson LECs from Tab. I. m_\star is set to $m_\star^{num} = 1150$ MeV in the expressions for $f_B^{(1,\nu)}$, eliminating the dependence of these quantities on m_0 (compare eq. (68)), while F_\star is varied in the range (112 ± 30) MeV to get an estimate for the error of the determined combinations (one finds that the results are not very sensitive to the choice of $2B_0\bar{m}$). The results of these fits are given in the tables below, for some given values of m_0 and F_\star , and for all four parameter sets of b_{1-11} from Tab. II. Based on the experience with these fits, and on the expectation of higher order corrections to the approximations made in eqs. (73), we can impose the following bounds on the parameter combinations in question (in appropriate units, specified in the above tables):

$$0.05 \leq \tilde{b}_D \leq 0.15, \tag{75}$$

$$-0.50 \leq \tilde{b}_F \leq -0.25, \tag{76}$$

$$-1.50 \leq \tilde{b}_0 \leq -0.20, \tag{77}$$

TABLE III: b_{1-11} from set 1

F_\star (MeV)	m_0 (MeV)	\tilde{b}_D (GeV $^{-1}$)	\tilde{b}_F (GeV $^{-1}$)	\tilde{b}_0 (GeV $^{-1}$)	\tilde{d}_7 (GeV $^{-3}$)
112	800	0.078	-0.352	-0.888	-0.158
112	1000	0.078	-0.352	-0.764	-0.168
112	1200	0.078	-0.352	-0.639	-0.180
80	800	0.109	-0.434	-1.158	-0.257
80	1000	0.109	-0.434	-1.067	-0.271
80	1200	0.109	-0.434	-0.974	-0.287
140	1000	0.066	-0.306	-0.599	-0.118

TABLE IV: b_{1-11} from set 2

F_\star (MeV)	m_0 (MeV)	\tilde{b}_D (GeV $^{-1}$)	\tilde{b}_F (GeV $^{-1}$)	\tilde{b}_0 (GeV $^{-1}$)	\tilde{d}_7 (GeV $^{-3}$)
112	800	0.062	-0.355	-0.961	-0.173
112	1000	0.062	-0.355	-0.838	-0.183
112	1200	0.062	-0.355	-0.713	-0.195
80	800	0.088	-0.437	-1.270	-0.277
80	1000	0.088	-0.437	-1.179	-0.291
80	1200	0.088	-0.437	-1.086	-0.307
140	1000	0.054	-0.308	-0.652	-0.130

$$-0.35 \leq \tilde{d}_7 \leq -0.05. \quad (78)$$

The parameter combinations $\tilde{b}_{D,F}$ will be fixed in the full fits for every set 1 – 4, while m_0, b_0, d_{1-7} will be left free - the comparison with the values \tilde{b}_0, \tilde{d}_7 from the tables above will only serve as a consistency check afterwards. Please note that the numerical values given in the previous four equations relate to the fixed values for μ and $2B_0\bar{m}$ specified above.

TABLE V: b_{1-11} from set 3

F_\star (MeV)	m_0 (MeV)	\tilde{b}_D (GeV $^{-1}$)	\tilde{b}_F (GeV $^{-1}$)	\tilde{b}_0 (GeV $^{-1}$)	\tilde{d}_7 (GeV $^{-3}$)
112	800	0.083	-0.358	-1.024	-0.181
112	1000	0.083	-0.358	-0.900	-0.192
112	1200	0.083	-0.358	-0.775	-0.203
80	800	0.117	-0.443	-1.362	-0.289
80	1000	0.117	-0.443	-1.271	-0.303
80	1200	0.117	-0.443	-1.178	-0.319
140	1000	0.069	-0.310	-0.697	-0.136

TABLE VI: b_{1-11} from set 4

F_\star (MeV)	m_0 (MeV)	\tilde{b}_D (GeV $^{-1}$)	\tilde{b}_F (GeV $^{-1}$)	\tilde{b}_0 (GeV $^{-1}$)	\tilde{d}_7 (GeV $^{-3}$)
112	800	0.072	-0.305	-0.504	-0.091
112	1000	0.072	-0.305	-0.380	-0.101
112	1200	0.072	-0.305	-0.255	-0.113
80	800	0.095	-0.365	-0.580	-0.166
80	1000	0.095	-0.365	-0.490	-0.180
80	1200	0.095	-0.365	-0.396	-0.196
140	1000	0.063	-0.271	-0.322	-0.068

Full one-loop fits to the fan plots

In the next step, we use the full one-loop expressions for the baryon masses in the fit functions. We fit to the fan plot data for the baryon octet masses (Table 22 of [35]) and the lowest three points for $X_N(\bar{m}, \nu = 0) = m_\star(M_\star)$ (from Table 19 of [35]) where $M_\star \leq 412$ MeV. In addition, we require that $X_N(\nu) \approx 1150$ MeV for $\nu \in \{-0.692, -0.558, -0.404, -0.275, -0.128, 0, 0.181\}$ (i.e. at the fan plot data points), where we allow for an error of 10% for $X_N(\nu)$ at those points. $m_\star(M_\star)$ is derived from eq. (71) with the help of eq. (8). Throughout we eliminate F_0 in favor of F_\star - the differ-

ence, however, formally amounts to an $\mathcal{O}(p^5)$ -effect in the baryon masses, which is beyond the order we are working in. The ratios f_B are directly obtained by inserting the one-loop expressions for the baryon masses, without further expansion in ν or \bar{m} . Also, $X_N(\nu)$ is not truncated after $\mathcal{O}(\nu^2)$ in the full fits. In the fan plot fitting functions, including $X_N(\nu)$, where the average quark mass is fixed to its physical value, we shall use the numerical values from eqs. (23, 24). The meson-LECs will be taken from the MILC2010 set, see Tab. I. The two combinations $\tilde{b}_{D,F}$ will then be fixed to the corresponding values determined in the previous subsection, for each of the four sets of b_{1-11} from Tab. II.

With given values for $\tilde{b}_{D,F}$ for $\sqrt{2B_0\bar{m}} = 0.42 \text{ GeV}$, we can determine seven more parameters from the present data set. First, the $(\delta m_\ell)^2$ -terms in the baryon mass formulae can be fixed by four free parameters, which may be taken as

$$\tilde{d}_1 := d_1 - \frac{1}{3}d_3, \quad d_2, \quad \tilde{d}_4 := d_4 + \frac{4}{3}d_3 \quad (79)$$

(see e.g. eq. (63)) and \tilde{d}_7 defined in eq. (74). Furthermore, inserting

$$b_D = \tilde{b}_D - 8(0.42 \text{ GeV})^2 d_3 \quad (80)$$

in eq. (71), we can determine the combinations

$$\begin{aligned} b'_0 &:= b_0 - \frac{16}{3}(0.42 \text{ GeV})^2 d_3, \\ \tilde{d}_6 &:= \frac{4}{9}d_3 + d_6 + \frac{1}{3}d_7 \end{aligned} \quad (81)$$

and m_0 from the running of $X_N(\delta m_\ell = 0)$ with $B_0\bar{m}$. The combination \tilde{b}_0 used in the previous subsection can then be computed, for $\sqrt{2B_0\bar{m}} = 0.42 \text{ GeV}$, as

$$\tilde{b}_0 = b'_0 + 12B_0\bar{m}\tilde{d}_6. \quad (82)$$

The results are given below, in Tab. VII. The fits are very good, $\chi^2/\text{d.o.f.} \sim 0.2$. This can be understood from the fact that the fan plots look very linear near the symmetric point, and the linear approximation fixed by the parameter combinations $\tilde{b}_{D,F}$ already describes this part quite well - better than one could have expected beforehand. Moreover, we have enough free LECs at hand to describe the behavior of X_N in a satisfying manner. The emerging fitting parameters are all of natural size, and $m_0 \sim 1 \text{ GeV}$. In the fits leading to the results in Tab. VIII, we have also included the physical (experimental) values for the baryon masses in the fit, assigning an error of 5 MeV to each due to our neglect of isospin-breaking

effects. The baryon masses at the physical point are obtained inserting $\nu = -0.885$ and our standard value for $2B_0\bar{m}$ in our mass formulae. As a consistency check of our procedure, we have also performed the fits without the constraints on $\tilde{b}_{D,F}$. The corresponding results can be found in Tab. IX and Tab. X. To get an estimate of the stability of our results due to uncertainties in the input values and higher order corrections, we have also performed full fits where the meson decay constant is strictly truncated to the value F_0 of the MILC2010 set of LECs, see Tab. I. The fit parameters following with this input can be read off from Tab. XI. We observe a good overall agreement of all these fits: varying the input parameters b_i, F_*, L_i always leads to similar results. We will discuss our results in detail in the next section.

TABLE VII: Results for the fit parameters. The set-number refers to Tab. II. $\tilde{b}_{D,F}$ are fixed input. m_0 is given in GeV, $b'_0, \tilde{b}_{D,F}$ in GeV^{-1} , and the d_i are given in GeV^{-3} at a scale $\mu = 1150 \text{ MeV}$. Here, the experimental masses are not included in the fit.

set	\tilde{b}_D	\tilde{b}_F	m_0	b'_0	\tilde{d}_1	d_2	\tilde{d}_4	\tilde{d}_6	\tilde{d}_7	\tilde{b}_0
1	0.078	-0.352	1.029	-0.364	0.035	0.122	0.020	-0.532	-0.244	-0.927
2	0.062	-0.355	1.051	-0.373	0.040	0.126	0.018	-0.603	-0.272	-1.011
3	0.083	-0.358	1.064	-0.400	0.030	0.121	0.030	-0.641	-0.289	-1.078
4	0.072	-0.305	0.930	-0.271	0.025	0.101	0.042	-0.213	-0.113	-0.497

TABLE VIII: Results for the fit parameters. Here, the fit includes the experimental baryon masses.

set	\tilde{b}_D	\tilde{b}_F	m_0	b'_0	\tilde{d}_1	d_2	\tilde{d}_4	\tilde{d}_6	\tilde{d}_7	\tilde{b}_0
1	0.078	-0.352	1.026	-0.370	0.035	0.046	0.044	-0.525	-0.257	-0.926
2	0.062	-0.355	1.046	-0.381	0.041	0.050	0.041	-0.594	-0.287	-1.010
3	0.083	-0.358	1.058	-0.411	0.030	0.047	0.054	-0.630	-0.306	-1.077
4	0.072	-0.305	0.936	-0.262	0.024	0.017	0.063	-0.222	-0.115	-0.496

TABLE IX: Consistency check. Here, the combinations $\tilde{b}_{D,F}$ are not fixed, and the experimental masses are not included in the fit. The values for \tilde{b}_0, \tilde{b}_F are computed for each set of fit results.

set	m_0	b'_0	\tilde{b}_D	b'_F	\tilde{d}_1	d_2	\tilde{d}_4	\tilde{d}_6	\tilde{d}_7	\tilde{b}_0	\tilde{b}_F
1	1.028	-0.372	0.087	-0.405	0.043	0.119	0.039	-0.531	-0.244	-0.933	-0.321
2	1.050	-0.381	0.072	-0.409	0.048	0.122	0.036	-0.602	-0.273	-1.017	-0.323
3	1.063	-0.407	0.092	-0.412	0.040	0.121	0.051	-0.640	-0.289	-1.084	-0.327
4	0.929	-0.278	0.079	-0.346	0.033	0.095	0.059	-0.211	-0.114	-0.501	-0.280

TABLE X: Consistency check. Here, the fit includes the experimental baryon masses, but the combinations $\tilde{b}_{D,F}$ are not fixed.

set	m_0	b'_0	\tilde{b}_D	b'_F	\tilde{d}_1	d_2	\tilde{d}_4	\tilde{d}_6	\tilde{d}_7	\tilde{b}_0	\tilde{b}_F
1	1.021	-0.378	0.077	-0.357	0.039	0.022	0.051	-0.518	-0.257	-0.926	-0.341
2	1.042	-0.389	0.062	-0.361	0.044	0.025	0.048	-0.587	-0.287	-1.010	-0.343
3	1.054	-0.417	0.082	-0.365	0.035	0.025	0.062	-0.624	-0.305	-1.077	-0.347
4	0.930	-0.269	0.069	-0.295	0.027	0.010	0.067	-0.213	-0.115	-0.494	-0.302

VII. DISCUSSION

Convergence at the symmetric point

We start the discussion of our results with the singlet sector where $\delta m_\ell = 0$. Let us have a look at the expansion of m_\star , using the parameter sets from Tab. VII as typical examples. The dimensionless suppression factor could naively be expected to be of the order

$$\frac{\sqrt{2B_0\bar{m}}}{4\pi F_\star} \sim \frac{420}{4\pi \cdot 112} \sim 0.3. \quad (83)$$

Of course, we already know, e.g. from the considerations in sec. IV, that the leading nonanalytic loop correction $\sim M^3$ is much enhanced w.r.t. this expectation. Using eq. (71), we

TABLE XI: Stability check. Here we use the value from MILC2010 for the meson decay constant as input everywhere, instead of F_\star . The fit includes the experimental baryon masses, but the combinations $\tilde{b}_{D,F}$ are not fixed.

set	m_0	b'_0	\tilde{b}_D	b'_F	\tilde{d}_1	d_2	\tilde{d}_4	\tilde{d}_6	\tilde{d}_7	\tilde{b}_0	\tilde{b}_F
1	1.116	-0.329	0.118	-0.470	0.075	0.121	0.134	-1.247	-0.524	-1.649	-0.385
2	1.144	-0.337	0.097	-0.476	0.084	0.129	0.123	-1.411	-0.583	-1.831	-0.385
3	1.161	-0.371	0.126	-0.482	0.067	0.127	0.157	-1.500	-0.618	-1.960	-0.392
4	0.993	-0.211	0.098	-0.381	0.048	0.063	0.152	-0.516	-0.250	-0.757	-0.336

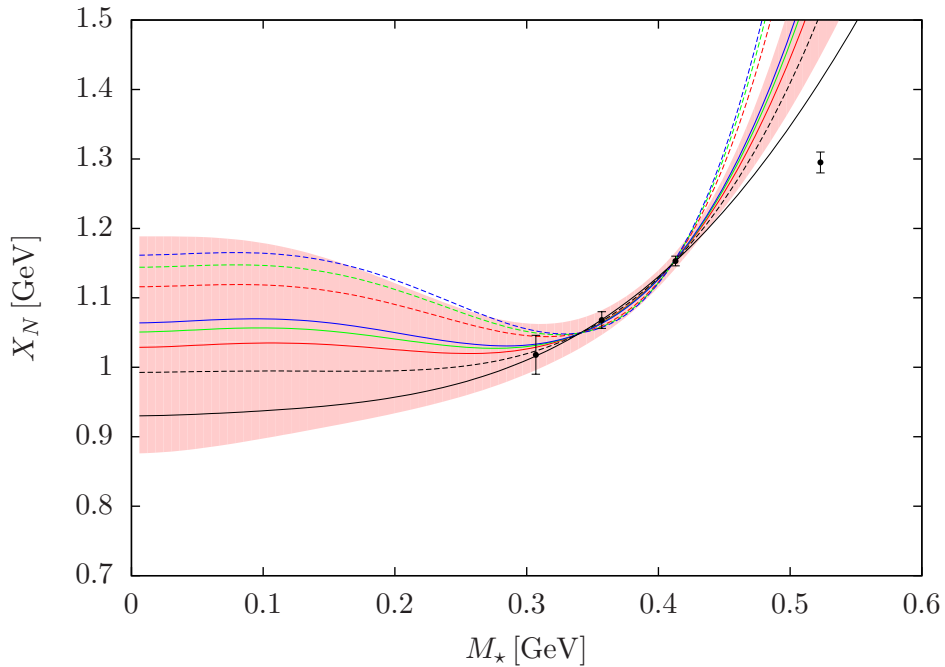


FIG. 4: The function $m_\star(M_\star)$ for the four parameter sets from Tab. VII (full lines) and from Tab. XI (dashed lines). Red: set 1, green: set 2, blue: set 3, black: set 4. The band shown here is the one-sigma error band pertaining to the full red curve.

find

$$\begin{aligned}
 m_\star &= m_0 - 4B_0\bar{m}(3b_0 + 2b_D) - (2B_0\bar{m})^{3/2} \frac{(5D^2 + 9F^2)}{24\pi F_\star^2} + \frac{(2B_0\bar{m})^2}{3(4\pi F_\star)^2} \left[\dots \right] + \mathcal{O}(\bar{m}^{5/2}) \\
 &\rightarrow (1029 + 330 - 397 + 186) \text{ MeV} = 1148 \text{ MeV} \quad \text{for set 1 from Tab. VII,}
 \end{aligned}$$

$$\begin{aligned}
&\rightarrow (1051 + 351 - 397 + 143) \text{ MeV} = 1148 \text{ MeV} && \text{for set 2 from Tab. VII,} \\
&\rightarrow (1064 + 365 - 397 + 115) \text{ MeV} = 1147 \text{ MeV} && \text{for set 3 from Tab. VII,} \\
&\rightarrow (930 + 236 - 397 + 380) \text{ MeV} = 1149 \text{ MeV} && \text{for set 4 from Tab. VII.}
\end{aligned}$$

The result for m_\star is very close to m_\star^{num} in all cases due to the constraint included in the fit. The coefficient in square brackets giving the fourth order contribution can be read off from eq. (71). We see that the observed convergence behavior is still inconclusive, though the fourth order contributions employing the LECs b_{1-11} from the meson-baryon scattering amplitudes are roughly in line with a suppression factor of ~ 0.5 . A similar pattern (at physical quark masses) has e.g. been found in [28], where some fourth order effects were estimated. In contrast, the fits for $b_{1-11} = 0$ result in expansions of m_\star which seem meaningless in the sense of perturbation theory.

To further study the convergence issue, we set the average quark mass to $2B_0\bar{m} = (300 \text{ MeV})^2$ (this entails $F_\star \rightarrow 104 \text{ MeV}$ using eq. (19)). Then we would have

$$\begin{aligned}
m_\star &\rightarrow (1029 + 169 - 168 - 10) \text{ MeV} = 1020 \text{ MeV} && \text{for set 1 from Tab. VII,} \\
m_\star &\rightarrow (1051 + 179 - 168 - 39) \text{ MeV} = 1023 \text{ MeV} && \text{for set 2 from Tab. VII,} \\
m_\star &\rightarrow (1064 + 186 - 168 - 57) \text{ MeV} = 1025 \text{ MeV} && \text{for set 3 from Tab. VII,} \\
m_\star &\rightarrow (930 + 120 - 168 + 122) \text{ MeV} = 1004 \text{ MeV} && \text{for set 4 from Tab. VII.}
\end{aligned}$$

The third order term is still comparatively large, cancelling most of the second order corrections, but the fourth order contributions already seem to be well under control for this low average quark mass. Unfortunately, there is no data available for such low average quark masses yet.

The parameters which are mostly determined from the behavior of the singlet sector can therefore not be fixed very accurately from the data set considered here. In particular, m_0, b'_0 and \tilde{d}_6 will be subject to large uncertainties. This also reflects itself in the following experiment: Including also the fourth data point for $m_\star(M_\star)$ at $M_\star \sim 530 \text{ MeV}$ in the fit, we observe that the aforesaid three parameters vary rather drastically (e.g. the results of Tab. VII shift to $m_0 \sim 800 \text{ MeV}$, $b'_0 \sim -0.9 \text{ GeV}^{-1}$, $\tilde{d}_6 \sim 0.04 \text{ GeV}^{-3}$), while the remaining parameters remain roughly the same. This is particularly disturbing for m_0 , a constant that reappears everywhere in three-flavor chiral extrapolations for baryon observables. We would like to point out that it would be very helpful for this purpose to have some more m_\star -data

points for $M_\star < 300 \text{ MeV}$. Up to now, we can only give the following very rough bounds, based on Tab. VII-XI and the variation of the input parameters:

$$800 \text{ MeV} \leq m_0 \leq 1200 \text{ MeV}, \quad (84)$$

$$-1 \text{ GeV}^{-1} \leq b'_0 \leq 0 \text{ GeV}^{-1}, \quad (85)$$

$$-2 \text{ GeV}^{-3} \leq \tilde{d}_6 \leq 0.50 \text{ GeV}^{-3}. \quad (86)$$

As a consequence of the results in Tab. XI, we revise the lower limit for the allowed range of the combination \tilde{b}_0 (see eq. (77)),

$$-2 \text{ GeV}^{-1} \leq \tilde{b}_0 \leq -0.20 \text{ GeV}^{-1}. \quad (87)$$

In Fig. 4, we show m_\star as a function of M_\star . One immediately sees that the uncertainty grows rapidly above the region where the curves are fixed by the fit to data (note that the fourth data point shown here is not included in the fits). Recall that *the only difference* between the fits leading to the full and the dashed curves in this figure is the $\mathcal{O}(p^5)$ -effect $F_\star \rightarrow F_0$. Beyond $M_\star \gtrsim 500 \text{ MeV}$, this higher-order effect has a very large impact on m_\star . Of course one could obtain good fits to lattice data in this region with both choices for the decay constant, but in our opinion, these fits would not be reliable in the sense of a stable determination of the fitting parameters (LECs). The finding that chiral extrapolations should not be trusted for meson masses much above 500 MeV is consistent with related studies [8, 52]. Beyond this regime, the extrapolations depend very strongly on the details of the input and fine-tuning of input and fitting parameters.

Symmetry breaking

Let us now discuss the parameters which determine the SU(3) symmetry breaking visualized by the fan plots, as seen in Fig. 5. First, it is reassuring to observe that it does not matter whether $\tilde{b}_{D,F}$ are used as fixed input in the full fits or not: Tables VII and IX and Tables VIII and X are very similar, even though the input values in Tab. VII and VIII were obtained with approximations linear in the variable ν for the ratios f_B and a quadratic approximation for X_N , and truncated chiral expansions for f_B (eq. (68)), including a re-ordering of terms to eliminate m_0 in favor of m_\star in the ratios. The bounds from the linear fits given in eqs. (75,76) are respected in all our resulting parameter sets. Even a rather

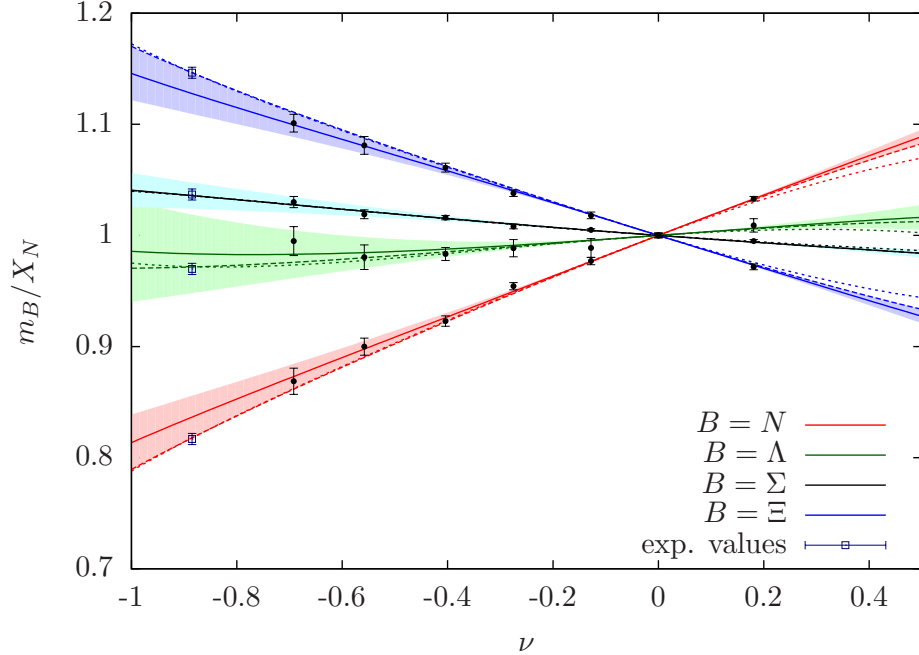


FIG. 5: Three different results for the fan plot curves, with b_{1-11} from set 1. Full line: from Tab. VII, dashed line: from Tab. VIII, dotted line: from Tab. X. The bands shown here are the one-sigma error bands pertaining to the full line. Recall that the fits corresponding to the dashed and dotted lines include the experimental baryon masses.

large variation of the meson decay constant (from $F_\star \sim 112$ MeV to $F_0 \sim 80$ MeV) does not invalidate this picture, as can be seen from the fourth and the last column of Tab. XI. It is also interesting to note that the combination $\frac{20}{3}\tilde{b}_D - \tilde{b}_F$ falls into the bound given in eq. (37) for $b_{D,F}$ for all fits from Tabs. VII-X, and is slightly above that range for the fits with set 1-3 from Tab. XI. From all these observations we can conclude that the determination of the LEC combinations parameterizing the linear part of the flavor symmetry breaking is very stable, thanks to the impressive new data leading to the fan plots. This is also illustrated by the error band and the three different fit curves shown in Fig. 5.

It remains to discuss the parameters determined from the nonlinear symmetry breaking effects. They appear at fourth chiral order in our formulae, which is the highest order we can compute exactly within the present one-loop framework. Therefore, we cannot expect a very high precision here. From our results, we extract the following allowed ranges for the

remaining parameter combinations (in units of GeV^{-3}):

$$-0.05 \leq \tilde{d}_1 \leq 0.15, \quad (88)$$

$$0.00 \leq d_2 \leq 0.25, \quad (89)$$

$$-0.10 \leq \tilde{d}_4 \leq 0.20, \quad (90)$$

$$-0.75 \leq \tilde{d}_7 \leq -0.05. \quad (91)$$

We stress again that these estimates concern the numerical values of the renormalized LECs at $\mu = 1150 \text{ MeV}$, and should be evolved by eqs. (52) when using infrared regularization at a different scale μ .

Obviously, the purely linear fits lead to an underestimation of the uncertainty in \tilde{d}_7 : Here we had to shift the lower limit of our previous constraint, mostly due to the fit results shown in Tab. XI, compare eqs. (78) and (91). In Fig. 6, we show the constrained behavior of the function $X_N(\nu)$, which is mostly secured by the combination \tilde{d}_7 . Here, the expectation of convergence at low orders *must* fail because the higher order terms in eq. (72) have to compensate for the leading ($\mathcal{O}(p^3)$) effect. This might partly explain why the range for \tilde{d}_7 in eq. (91) turns out to be comparatively broad.

Including the experimental masses in the fit mainly (and strongly) affects the result for d_2 , which parameterizes the curvature of the fan plot curves for the Ξ and the nucleon, compare e.g. Tab. VII and Tab. VIII, and the full versus the dashed and dotted curves in Fig. 5. While in all cases d_2 is of natural size, this shows that a reliable chiral extrapolation to the physical point, using one-loop BChPT expressions together with fan plot data, must still be considered problematic, in spite of the improvements in determining many LEC combinations worked out in the present contribution. In the framework of Heavy-Baryon ChPT, the low-energy constants d_{1-7} have been estimated from the resonance saturation principle, combined with a fit to experimental masses and sigma terms, by Borasoy and Meißner [3], see their eq. (68). Setting $\beta_R = 0$ in those equations, and forming our preferred combinations, we see that their results for $\tilde{d}_{1,4,7}$ and d_2 all lie in the ranges given above (their \tilde{d}_6 , however, is much smaller than in our tables, $\tilde{d}_6^{BM} = -0.022 \text{ GeV}^{-3}$). Moreover, according to their estimates, $\tilde{b}_D^{BM} = 0.176 \text{ GeV}^{-1}$ is somewhat above our allowed range (see eq. (75)), while their $\tilde{b}_F^{BM} = -0.344 \text{ GeV}^{-1}$ again agrees very well with our typical fit results. One should note that such a comparison can only be of qualitative nature, for various reasons. Besides the differences of the schemes and the issue of scale dependence, it is not known

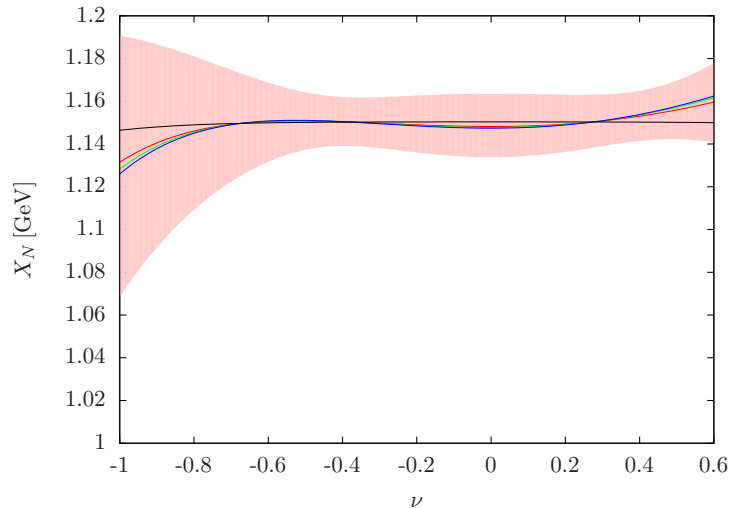


FIG. 6: The function $X_N(\nu)$ for the four fits of Tab. VII. Red: set 1, green: set 2, blue: set 3, black: set 4. The band shown here is the one-sigma error band pertaining to the red line.

how accurate the estimates from resonance saturation can probably be here, in particular because these LECs are not of “dynamical” nature (see also the discussion in sec. 5.2 of [21]). What is more, the masses and $\sigma_{\pi N}(0) = 45$ MeV at the physical point have been input in the estimates of [3], and we have already seen that in general the convergence properties of the chiral expansions are far from satisfying there due to the large m_s -corrections.

In [31], several parameterizations for the baryon masses were used to test the model dependence of the resulting fits to lattice data, and of the determination of the sigma terms. While this model dependence is found to be an important source of systematic uncertainty, we note that the LECs $b_{0,D,F}$ obtained from the $\mathcal{O}(p^3)$ -BChPT approach in [31] agree very well with the values we find for the corresponding parameters $\tilde{b}_{0,D,F}$ in our analysis.

Note added

Shortly after a first version of the present work appeared on the web, two other analyses of the lattice data discussed here became available [17, 34]. Of those, [34] uses a framework similar to the one used here (which is essentially given in [21]). It therefore seems reasonable to attempt a comparison of the resulting fitting parameters, though there is still a minor difference in the renormalization schemes used. Let us first have a look at the most important parameter in the singlet sector, the baryon mass in the chiral limit. The range of possible

values for this parameter we found is quite broad, see eq. (84). In Tab. XII we show their result in the first column, together with those of three other references in which this parameter is determined. We see that only the result of [30] is not in line with our broad estimate. Going on to the other LECs, and forming the combinations determined here with

TABLE XII: Results for m_0 (in GeV) from ref. [34] and three other references. For our estimate, see eq. (84).

Ref.	[34], Fit I	[30]	[32]	[3]
m_0	0.880 ± 0.022	0.756 ± 0.032	0.944 ± 0.002	0.767 ± 0.110

the results given in Table 6 (Fit I) of [34], we note that they are all consistent with the ranges we gave above, at least within the errors given there, with one exception, which is given by \tilde{b}_D (we have checked that the shift from $\mu = 1$ GeV used in the latter reference to the value $\mu = 1.15$ GeV used here does not induce large effects on our ranges). However, one should note that the parameter b_D in [34] jumps from a small value $\sim 0.05/\text{GeV}$ at $\mathcal{O}(p^2)$ and $\mathcal{O}(p^3)$ (consistent with our bounds on \tilde{b}_D) to a comparatively large value $\sim 0.22/\text{GeV}$ in the $\mathcal{O}(p^4)$ fits. We suppose that this parameter is particularly afflicted by convergence problems, given that a large part of the data set analysed in [34] are at the border, or even outside, of the region where the three-flavor expansions work in a reliable manner.

Sigma term

Rewriting our formula for the contact term contribution to the sigma term, eq. (48), in terms of our fitting parameters defined in eqs.(74,81), we find

$$\sigma_{\pi N}^{(ct)}(0) = -2B_0 m_\ell \left(4b'_0 + 2\tilde{b}_D + 2\tilde{b}_F + 96B_0 \tilde{m} \tilde{d}_6 + \frac{16}{3} (B_0 \delta m_\ell) (3\tilde{d}_1 + 3d_2 - 4d_3 + 9d_5 + 6\tilde{d}_7) \right). \quad (92)$$

This shows that we can write the sigma term resulting from our formulae as

$$\begin{aligned} \sigma_{\pi N}(0) &= \sigma_{\pi N}(0)|_{d_3=d_5=0} + \frac{8}{3} (2B_0 \delta m_\ell) (2B_0 m_\ell) (9d_5 - 4d_3) \\ &\approx \sigma_{\pi N}(0)|_{d_3=d_5=0} - \frac{8}{3} M_\pi^2 (X_\pi^2 - M_\pi^2) (9d_5 - 4d_3), \end{aligned} \quad (93)$$

where the first term is written in terms of our fitting parameters. The unknown constants d_3, d_5 parameterize the dependence on \bar{m} of the terms linear in δm_ℓ . The latter dependence starts as soon as one includes chiral loops, i.e. at $\mathcal{O}(p^3)$, see e.g. eq. (68). Let us consider two examples to estimate the unknown parameter combination in question, ignoring the issue of convergence for the moment. For the fit of Table VII with set 1, the first term is $\sigma_{\pi N}(0)|_{d_3=d_5=0} = 67 \text{ MeV}$, while for the fit with set 4, it results in 47 MeV . For the remainder, we can only give a very rough estimate based on a consistency condition: Requiring that the terms $\sim d_3, d_5$ do not yield more than a 100% correction in the combinations \tilde{b}_D, b'_F gives bounds $|d_3| \lesssim 0.07 \text{ GeV}^{-3}$ and $|d_5| \lesssim 0.38 \text{ GeV}^{-3} \Rightarrow -0.41 \lesssim (d_5 - \frac{4}{9}d_3) \text{ GeV}^3 \lesssim 0.41$, which produces sigma terms between $39 \dots 95 \text{ MeV}$ for set 1 and $19 \dots 75 \text{ MeV}$ for set 4. These bounds are consistent with recent three-flavor lattice determinations, see e.g. [31, 53]. We also mention that the above consistency bounds for $d_{3,5}$ are obeyed by the results for these two parameters given in [34].

However, it is to be noted that we do not see a clear sign of convergence for the sigma term at physical quark masses, so one should not overinterpret these last results. Basically we have to conclude that the sigma term could only be reliably determined from BChPT extrapolations when more data also for smaller average quark masses (so that e.g. $M_\star \sim 300 \text{ MeV}$) become available.

VIII. CONCLUSIONS

In summary, we have analyzed lattice data for octet baryon masses from [35] employing manifestly covariant BChPT with three dynamical flavors. We were able to give bounds on the numerical values of certain combinations of low-energy constants (LECs), which are, in our opinion, more reliable and accurate than it was possible before data for fixed average quark mass became available in [35]: As we have seen, the simulation strategy used in that work offers some advantages for this purpose. Eqs. (75,76), (84,85,86) and (88,89,90,91) should be considered as our main results. We hope that these bounds will be useful in the near future, e.g. when studying the chiral behavior of other hadron observables with the same simulation strategy. Though we have fixed the running of the baryon masses on the two trajectories $\{\bar{m} = \text{const.}, \delta m_\ell\}$ and $\{\bar{m}, \delta m_\ell = 0\}$, there are still two undetermined parameters, chosen here as d_3 and d_5 , which would have to be fixed in order to make an $\mathcal{O}(p^4)$

prediction for the sigma term. However, even if those parameters were fixed accurately, the uncertainty in the determination of the sigma term would still be very large due to the very slow convergence near the physical point. For an investigation of sigma terms, a two-flavor version of ChPT is certainly superior; we refer to [54] for a recent determination. In closing, we stress again that additional data points for lower average quark masses would be very helpful in order to reach a truly controlled chiral extrapolation.

Acknowledgments

We acknowledge discussions and useful communications with G. Bali, M. Frink, M. Mai, U.-G. Meißner, P. E. L. Rakow, A. Rusetsky and A. Sternbeck. This work was supported by the Deutsche Forschungsgemeinschaft SFB/Transregio 55. L. G. acknowledges support by the European Union under Grant Agreement number 256594 (IRG).

-
- [1] E. E. Jenkins and A. V. Manohar, Phys. Lett. B **255** (1991) 558.
 - [2] A. Krause, Helv. Phys. Acta **63** (1990) 3, <http://retro.seals.ch>
 - [3] B. Borasoy and U. -G. Meißner, Annals Phys. **254** (1997) 192 [hep-ph/9607432].
 - [4] J. Gasser, In *Mainz 1997, Chiral dynamics: Theory and experiment* 12-25 [hep-ph/9711503].
 - [5] J. F. Donoghue and B. R. Holstein, hep-ph/9803312.
 - [6] J. F. Donoghue, B. R. Holstein and B. Borasoy, Phys. Rev. D **59** (1999) 036002 [hep-ph/9804281].
 - [7] M. Mojziz and J. Kambor, Phys. Lett. B **476** (2000) 344 [hep-ph/9912517].
 - [8] D. Djukanovic, J. Gegelia and S. Scherer, Eur. Phys. J. A **29** (2006) 337 [hep-ph/0604164].
 - [9] M. Mai, P. C. Bruns, B. Kubis and U. -G. Meißner, Phys. Rev. D **80** (2009) 094006 [arXiv:0905.2810 [hep-ph]].
 - [10] T. Meissner, Phys. Lett. B **340** (1994) 226 [hep-ph/9405289].
 - [11] A. Walker-Loud, H. -W. Lin, D. G. Richards, R. G. Edwards, M. Engelhardt, G. T. Fleming, P. Hagler and B. Musch *et al.*, Phys. Rev. D **79** (2009) 054502 [arXiv:0806.4549 [hep-lat]].
 - [12] K. -I. Ishikawa *et al.* [PACS-CS Collaboration], Phys. Rev. D **80** (2009) 054502 [arXiv:0905.0962 [hep-lat]].

- [13] A. Semke and M. F. M. Lutz, Nucl. Phys. A **778** (2006) 153 [nucl-th/0511061].
- [14] R. Flores-Mendieta, C. P. Hofmann, E. E. Jenkins and A. V. Manohar, Phys. Rev. D **62** (2000) 034001 [hep-ph/0001218].
- [15] A. Walker-Loud, Phys. Rev. D **86** (2012) 074509 [arXiv:1112.2658 [hep-lat]].
- [16] A. C. Cordon and J. L. Goity, arXiv:1209.0030 [hep-ph].
- [17] M. F. M. Lutz and A. Semke, Phys. Rev. D **86** (2012) 091502 [arXiv:1209.2791 [hep-lat]].
- [18] B. C. Tiburzi and A. Walker-Loud, Phys. Lett. B **669** (2008) 246 [arXiv:0808.0482 [nucl-th]].
- [19] F. -J. Jiang, B. C. Tiburzi and A. Walker-Loud, Phys. Lett. B **695** (2011) 329 [arXiv:0911.4721 [nucl-th]].
- [20] T. Becher, H. Leutwyler, Eur. Phys. J. **C9** (1999) 643-671. [hep-ph/9901384].
- [21] M. Frink and U. -G. Meißner, JHEP **0407** (2004) 028 [hep-lat/0404018].
- [22] P. J. Ellis and K. Torikoshi, Phys. Rev. C **61** (2000) 015205 [nucl-th/9904017].
- [23] E. E. Jenkins, Nucl. Phys. B **368** (1992) 190.
- [24] V. Bernard, N. Kaiser, U. -G. Meißner, Z. Phys. **C60** (1993) 111-120. [hep-ph/9303311].
- [25] R. F. Lebed and M. A. Luty, Phys. Lett. B **329** (1994) 479 [hep-ph/9401232].
- [26] A. Walker-Loud, Nucl. Phys. A **747** (2005) 476 [hep-lat/0405007].
- [27] M. Frink, U. -G. Meißner, I. Scheller, Eur. Phys. J. **A24** (2005) 395-409. [hep-lat/0501024].
- [28] B. C. Lehnhart, J. Gegelia and S. Scherer, J. Phys. G **31** (2005) 89 [hep-ph/0412092].
- [29] R. D. Young and A. W. Thomas, Phys. Rev. D **81** (2010) 014503 [arXiv:0901.3310 [hep-lat]].
- [30] J. Martin Camalich, L. S. Geng and M. J. Vicente Vacas, Phys. Rev. D **82** (2010) 074504 [arXiv:1003.1929 [hep-lat]].
- [31] S. Dürr, Z. Fodor, T. Hemmert, C. Hoelbling, J. Frison, S. D. Katz, S. Krieg and T. Kurth *et al.*, Phys. Rev. D **85** (2012) 014509 [arXiv:1109.4265 [hep-lat]].
- [32] A. Semke and M. F. M. Lutz, Phys. Rev. D **85** (2012) 034001 [arXiv:1111.0238 [hep-ph]].
- [33] A. Semke and M. F. M. Lutz, Phys. Lett. B **717** (2012) 242 [arXiv:1202.3556 [hep-ph]].
- [34] X. -L. Ren, L. S. Geng, J. M. Camalich, J. Meng and H. Toki, arXiv:1209.3641 [nucl-th].
- [35] W. Bietenholz, V. Bornyakov, M. Göckeler, R. Horsley, W. G. Lockhart, Y. Nakamura, H. Perlt and D. Pleiter *et al.*, Phys. Rev. D **84** (2011) 054509 [arXiv:1102.5300 [hep-lat]].
- [36] S. Aoki *et al.* [PACS-CS Collaboration], Phys. Rev. D **79** (2009) 034503 [arXiv:0807.1661 [hep-lat]].
- [37] S. Dürr, Z. Fodor, C. Hoelbling, S. D. Katz, S. Krieg, T. Kurth, L. Lellouch and T. Lippert

- et al.*, JHEP **1108** (2011) 148 [arXiv:1011.2711 [hep-lat]].
- [38] P. E. Shanahan, A. W. Thomas and R. D. Young, arXiv:1205.5365 [nucl-th].
- [39] J. Gasser and H. Leutwyler, Nucl. Phys. B **250** (1985) 465.
- [40] G. Colangelo, S. Dürr, A. Juttner, L. Lellouch, H. Leutwyler, V. Lubicz, S. Necco and C. T. Sachrajda *et al.*, Eur. Phys. J. C **71** (2011) 1695 [arXiv:1011.4408 [hep-lat]].
- [41] A. Bazavov *et al.* [MILC Collaboration], PoS LATTICE **2010** (2010) 074 [arXiv:1012.0868 [hep-lat]].
- [42] A. Bazavov *et al.* [MILC Collaboration], PoS CD **09** (2009) 007 [arXiv:0910.2966 [hep-ph]].
- [43] R. L. Jaffe and A. Manohar, Nucl. Phys. B **337** (1990) 509.
- [44] F. E. Close and R. G. Roberts, Phys. Lett. B **316** (1993) 165 [hep-ph/9306289].
- [45] B. Borasoy, Phys. Rev. D **59** (1999) 054021 [hep-ph/9811411].
- [46] H. -W. Lin and K. Orginos, Phys. Rev. D **79** (2009) 034507 [arXiv:0712.1214 [hep-lat]].
- [47] M. Gell-Mann, “The Eightfold Way: A Theory of strong interaction symmetry,” CTSL-20.
- [48] S. Okubo, Prog. Theor. Phys. **27** (1962) 949.
- [49] M. Frink, *private communication*, Dec. 2011.
- [50] P. C. Bruns, M. Mai and U. -G. Meißner, Phys. Lett. B **697** (2011) 254 [arXiv:1012.2233 [nucl-th]].
- [51] M. Mai, P. C. Bruns and U. -G. Meißner, Phys. Rev. D **86** (2012) 094033 [arXiv:1207.4923 [nucl-th]].
- [52] V. Bernard and U. -G. Meißner, Phys. Lett. B **639** (2006) 278 [hep-lat/0605010].
- [53] R. Horsley, Y. Nakamura, H. Perlt, D. Pleiter, P. E. L. Rakow, G. Schierholz, A. Schiller and H. Stuben *et al.*, Phys. Rev. D **85** (2012) 034506 [arXiv:1110.4971 [hep-lat]].
- [54] G. S. Bali, P. C. Bruns, S. Collins, M. Deka, B. Gläsle, M. Göckeler, L. Greil and T. R. Hemmert *et al.*, Nucl. Phys. B **866** (2013) 1 [arXiv:1206.7034 [hep-lat]].